

SAR COMPLIANCE TESTING OF ASKEY COMPUTER CORPORATION MODEL WLL220  
MINI PCI CARD BUILT INTO COMPAL MODEL BCL50 NOTEBOOK COMPUTER

FCC ID: H8NWLL220CL  
Host Computer: Compal Model BCL50

May 2, 2003

Prepared for: Askey Computer Corporation  
10 F, No. 119, Chienkang Road  
Chung-Ho, Taipei, Taiwan R.O.C.  
Attention: Mr. John Chiou/PTT Manager

Prepared by: Om P. Gandhi  
Professor of Electrical and Computer Engineering  
University of Utah  
50 S Central Campus Dr., Rm. 3280  
Salt Lake City, UT 84112-9206

## TABLE OF CONTENTS

I. Introduction .....	1
II. The SAR Measurement System .....	2
The Flat Phantom .....	3
III. Calibration of the E-Field Probe .....	3
IV. SAR System Verification .....	4
V. Tissue Simulant Fluid for the Frequency Band 5.2 to 5.8 GHz .....	6
VI. The Measured SAR Distributions.....	7
VII. Comparison of the Data with FCC 96-326 Guidelines .....	9
REFERENCES .....	10
TABLES .....	12-30
FIGURES .....	31-68
APPENDIX A .....	69
APPENDIX B .....	73

# SAR COMPLIANCE TESTING OF ASKEY COMPUTER CORPORATION MODEL WLL220 MINI PCI CARD BUILT INTO COMPAL MODEL BCL50 NOTEBOOK COMPUTER

FCC ID: H8NWLL220CL  
Host Computer: Compal Model BCL50

## I. Introduction

The U.S. Federal Communications Commission (FCC) has adopted limits of human exposure to RF emissions from mobile and portable devices that are regulated by the FCC [1]. The FCC has also issued Supplement C (Edition 97-01) to OET Bulletin 65 [2] and a more recent version of the same [3] defining both the measurement and the computational procedures that should be followed for evaluating compliance of mobile and portable devices with FCC limits for human exposure to radiofrequency emissions.

We have used the measurement procedure for SAR compliance testing of the Askey Corporation Model WLL220 Mini PCI Card built into Compal Model BCL50 Notebook Computer (FCC ID# H8NWLL220CL). The photographs of the Model BCL50 Notebook Computer with built-in Model WLL220 Mini PCI Card are given in Figs. 1a, b, c, and Fig. 2, respectively. As seen in Fig. 2, two 802.11a antennas marked "A" and "B" antennas are built close to the right and left edges of the keyboard, respectively. Even though two 802.11a antennas are built into the base of the PC for diversity, only one of the two antennas are active at any given time. Each of the Askey Model WLL220 802.11a wireless antennas operates over the frequency band 5.15 to 5.80 GHz in normal or turbo modes with conducted power levels given in Table 1.

For SAR measurements, two configurations of the wireless PC relative to the experimental phantom have been used. These are as follows:

- a. **Configuration 1** is for the wireless PC placed on a user's lap. For this configuration, a planar phantom model with inside dimensions 12" x 16.5" (30.5 x 41.9 cm) and a base thickness of  $2.0 \pm 0.2$  mm (recommended in [3]) was used for SAR measurements and

the bottom side of the laptop computer shown in Fig. 1b was pressed against it. The SARs were measured both for the "A" and "B" antennas individually (see Figs. 3a, b).

- b. **Configuration 2** -- Edge-on position. This configuration corresponds to a bystander close to the right or left edges of the PC base at a distance of 1.5 cm. For this configuration, the right or the left edge of the PC base is placed at  $90^\circ$  relative to the flat phantom at a distance of 1.5 cm as shown in Figs. 4a, b, respectively. As for Configuration 1, here too, the SARs were measured both for the "A" and "B" antennas individually (see Figs. 4a,b).

## II. The SAR Measurement System

The University of Utah SAR Measurement System has been described in peer-reviewed literature [Ref. 8 -- attached here as Appendix A]. A photograph of the SAR Measurement System is given in Fig. 5. This SAR Measurement System uses a computer-controlled 3-D stepper motor system (Arrick Robotics MD-2A). A triaxial Narda Model 8021 E-field probe is used to determine the internal electric fields. The positioning repeatability of the stepper motor system moving the E-field probe is within  $\pm 0.1$  mm. Outputs from the three channels of the E-field probe are dc voltages, the sum of which is proportional to the square of the internal electric fields  $\left(|E_i|^2\right)$  from which the SAR can be obtained from the equation  $SAR = \sigma \left(|E_i|^2\right) / \rho$ , where  $\sigma$  and  $\rho$  are the conductivity and mass density of the tissue-simulant materials, respectively [5]. The dc voltages for the three channels of the E-field probe are read by three HP 34401A multimeters and sent to the computer via an HPIB interface. The setup is carefully grounded and shielded to reduce the noise due to the electromagnetic interference (EMI). A cutout in a wooden table of dimensions  $38.1 \times 21.6$  cm allows placement of a plastic holder (shown in Fig. 6) on which the laptop computer with the 802.11 a/b wireless antennas (see Figs. 1 and 2) is supported. A plastic holder (see Fig. 6) can be moved up or down so that the base of the PC (for Configuration 1) is pressed against the base of the flat phantom for determination of SAR for Above-Lap position. Similarly, for "Edge-On" SAR determination, Configuration 2,

the laptop computer is mounted sideways (at  $90^\circ$ ) on the plastic holder and moved up so that the right or the left edge of the keyboard base with the 802.11 a/b "A" or "B" wireless antennas is at a distance of 1.5 cm from the bottom of the flat phantom (see Figs. 4a, b).

### **The Flat Phantom**

As recommended in Supplement C Edition 01-01 to OET Bulletin 65 [3], a planar phantom model with inside dimensions  $12" \times 16.5"$  ( $30.5 \times 41.9$  cm) and base thickness  $2.0 \pm 0.2$  mm was used for SAR measurements (see Figs. 3-5).

### **III. Calibration of the E-Field Probe**

The IEEE Draft Standard P1528 [4] suggests a recommended procedure for probe calibration (see Section 4.4.1 of [4]) for frequencies above 800 MHz where waveguide size is manageable. Calibration using a rectangular waveguide is recommended. As in some previously reported SAR measurements at 6 GHz [5], we have calibrated the Narda Model 8021 Miniature Broadband Electric Field Probe of tip diameter 4 mm (internal dipole dimensions on the order of 2.5 mm) using a rectangular waveguide WR 159 (of internal dimensions 1.59 x 0.795 inches) that was filled with the tissue-simulant fluid of composition given in Section V (see Figs. 7a, b). The triaxial (3 dipole) E-field probe shown in Fig. 8 was originally developed by Howard Bassen and colleagues of FDA and has been manufactured under license by Narda Microwave Corporation, Hauppauge, New York. The probe is described in detail in references 6 and 7. It uses three orthogonal pick up dipoles each of length about 2.5 mm offset from the tip by 3 mm, each with its own leadless zero voltage Schottky barrier diode operating in the square law region. The sum of the three diode outputs read by three microvoltmeters [8] gives an output proportional to  $E^2$ . By rotating the probe around its axis, the isotropy of the probe was measured to be less than  $\pm 0.23$  dB and the deviation of the probe from the square law behavior was less than  $\pm 3\%$ .

As suggested in the Draft Standard P1528, the waveguide (WR 159) filled with the tissue-simulant fluid was maintained vertically. From microwave field theory [see e.g. ref. 9],

the transverse field distribution in the liquid corresponds to the fundamental mode ( $TE_{10}$ ) with an exponential decay in the vertical direction ( $z$ -axis). The liquid level was 15 cm deep which is deep enough to guarantee that reflections from the top liquid surface do not affect the calibration. By comparing the square of the decaying electric fields expected in the tissue from the analytical expressions for the  $TE_{10}$  mode of the rectangular waveguide, we obtained a calibration factor of 2.98 (mW/kg)/ $\mu$ V with a variability of less than  $\pm 2\%$  for measurement frequencies of 5.25 and 5.8 GHz, respectively. This is no doubt due to a fairly limited frequency band of only 0.55 GHz out of a recommended bandwidth of 2.2 GHz for the  $TE_{10}$  mode for the WR159 waveguide (recommended band of 4.9-7.1 GHz -- see e.g. ref. 9) and the fact that the bandwidth of 550 MHz for the entire set of measurements is on the order of  $\pm 5\%$  of the midband frequencies..

The date for the calibration of the E-field probe closest to the SAR tests given here was April 28, 2003.

#### **IV. SAR System Verification**

It is very difficult to develop half wave dipole antennas for use in the 5.2 to 5.8 GHz band both because of fairly small dimensions and the resulting dimensional tolerances, and relatively narrow bandwidths of the required baluns – balanced-to-unbalanced transformers. On the other hand, waveguides are broadband with simultaneous bandwidths larger than 1-2 GHz and fairly easy to use for frequencies in excess of 3 GHz. As shown in Fig. 9, we have, therefore, developed a system verification system by using an open-ended, air-filled waveguide as an irradiation system placed at a distance of 8 mm from the base of the planar phantom (10 mm from the lossy fluid in the phantom). For this application, we have set up a WR 187 rectangular waveguide of internal dimensions 1.872"  $\times$  0.872" that is fed with microwave power from a Hewlett Packard Model 83620A Synthesized Sweeper (10 MHz-20 GHz). The operating ( $TE_{10}$  mode) band of this waveguide is from 3.95 to 5.85 GHz. The microwave circuit arrangement used for system verification is sketched in Fig. 10. When placed at a distance of 8 mm from the base of the planar phantom, the reflection coefficient is about 10-20%. As seen in

Fig. 9, even this relatively small amount of reflection has been reduced to less than 0.5% by using a movable slide-screw waveguide tuner (Narda Model 22CI). The measured SAR distributions for peak 1-g SAR region using this system at 5.25 and 5.80 GHz for the day of SAR measurements April 28, 2003 are given in Appendix A. Also given in Appendix A are the waveguide SAR plots for this date of SAR measurements. The peak 1-g SARs measured for 100 mW of radiated power for 5.25 and 5.80 GHz are 3.678 and 3.947 W/kg, respectively. The measured 1-g SARs are in excellent agreement with the FDTD-calculated 1-g SARs for this waveguide of 3.580 and 3.946 W/kg at 5.25 and 5.80 GHz, respectively. Also as expected, the measured SAR plots in Appendix A are quite symmetric at both of the irradiation frequencies.

For FDTD-calculations of the SAR distributions for the WR187 rectangular waveguide irradiation system, we have used the dielectric properties for the phantom given in Table 2 that have been taken from [3]. Using a resolution of 0.5 mm for the FDTD cells, the calculated variations of the SAR distributions are given in Figs. 11a, b as a function of height above the bottom surface of the phantom. From Figs. 11a, b, it is obvious that the penetration of electromagnetic fields in the 5.2-5.8 GHz range is extremely shallow. The calculated depths of penetration corresponding to  $1/e^2$ -reduction of SAR (13.5% of the SAR at the surface) are only 6.85 and 5.95 mm at 5.25 and 5.8 GHz, respectively. Both of these depths of penetration for this near-field exposure system are very similar to those obtained for plane wave irradiation at these frequencies (7.15 mm for 5.25 GHz and 6.25 mm for 5.8 GHz).

Also shown in Figs. 11a, b are the SAR variations measured for this waveguide exposure system at depths of 4, 6, 8, 10, 12, and 14 mm in the tissue-simulant fluid. We tried second-, third-, fourth-, and fifth-order polynomial least-square fits to extrapolate the measured SARs to depths of 1, 3, 5, 7, and 9 mm. As seen in Figs. 11a, b, the fourth-order polynomial provides an excellent agreement with the FDTD-calculated in-depth variation of SAR both at 5.25 and 5.8 GHz. Also as aforementioned, the peak 1-g SARs thus obtained for 100 mW of radiated power for 5.25 and 5.80 GHz of 3.678 and 3.947 W/kg are extremely close to the FDTD-calculated 1-g SARs for this waveguide of 3.580 and 3.946 W/kg at the two frequencies, respectively.

## V. Tissue Simulant Fluid for the Frequency Band 5.2 to 5.8 GHz

In OET 65 Supplement C [3], the dielectric parameters suggested for body phantom are given only for 3000 and 5800 MHz. These are listed in Table 2 here. Using linear interpolation, we can obtain the dielectric parameters to use for the frequency band between 5.25 to 5.8 GHz. The desired dielectric properties thus obtained are also given in Table 2. From Table 2, it can be noticed that the desired dielectric constant  $\epsilon_r$  varies from 48.2 to 49.0 which is a variation of less than  $\pm 1\%$  from the average value of 48.6 for this band. Also the conductivity  $\sigma$  varies linearly with frequency from 5.3 to 6.00 S/m. For the SAR measurements given in this report, we have used a tissue-simulant fluid developed at the University of Utah which consists of 68.0% water, 31.0% sugar and 1% HEC. For this composition, we have measured the dielectric properties using a Hewlett Packard (HP) Model 85070B Dielectric Probe in conjunction with HP Model 8720C Network Analyzer (50 MHz-20 GHz). The measured dielectric properties at a mid band frequency of 5.30 GHz are as follows:  $\epsilon_r = 48.5 \pm 1.7$  and  $\sigma = 5.40 \pm 0.08$  S/m. From Table 2, we obtain the desired dielectric properties to simulate the body tissue at the midband frequency of 5.30 GHz to be  $\epsilon_r = 48.9$  and  $\sigma = 5.42$  S/m. Thus, the measured properties for the body-simulant fluid are close to the desired values. Also as expected, the conductivity of this fluid varies linearly with frequency rising to  $6.03 \pm 0.09$  S/m at 5.8 GHz, while the dielectric constant  $\epsilon_r$  is nearly the same as the measured value at 5.3 GHz.

The procedure is as follows: The HP Model 95070B Dielectric Probe (see Fig. 12) is an open-circuited transmission-line (coaxial line) probe similar to that described in Section B.1.2 of the Draft IEEE Standard 1528 [4]. The theory of the open-circuited coaxial line method has been described in scientific literature [10-12]. We have previously used this method in determining the dielectric properties of tissue-simulant materials at 6 GHz [5]. In this method, the complex reflection coefficient  $\Gamma^*$  measured for the open end of the coaxial line can be used to calculate the complex permittivity  $\epsilon^*$  from the following equation [5]



$$\varepsilon^* = \frac{1 - \Gamma^*}{j\omega Z_o C_o (1 + \Gamma^*)} - \frac{C_f}{C_o} \quad (1)$$

where  $Z_o$  is the characteristic impedance ( $50 \Omega$ ) for the coaxial line,  $C_o$  is the capacitance when the line is in air and  $C_f$  is the capacitance that accounts for the fringing fields in the dielectric of the coaxial line.

For the HP85070B Dielectric Probe with diameters of the outer and inner conductors  $2b = 3.00$  mm and  $2a = 0.912$  mm, respectively, the following capacitances were obtained using deionized water and methanol as the calibration fluids. The following capacitances were obtained:

$$C_o = 0.022 \text{ pF}$$

$$C_f = 0.005 \text{ pF}$$

Using the network analyzer HP8720C, we measured the reflection coefficient  $\Gamma^*$  for the open end of the coaxial line that was submerged in the tissue-simulant fluid. Using Eq. 1, the complex permittivity of the fluid was measured at various frequencies 5.2-5.4 GHz. From the imaginary part of the complex permittivity  $\text{Im}(\varepsilon^*)$ , we can obtain the conductivity  $\sigma$  from the relationship

$$\sigma = \frac{\text{Im}(\varepsilon^*)}{\omega \varepsilon_o} \quad (2)$$

## VI. The Measured SAR Distributions

The RF power output measured for the Askey Model WLL220 802.11a Wireless Antenna is given in Table 1. For SAR measurements, we selected frequencies of 5.26 GHz and 5.805 GHz for the normal mode and 5.29 and 5.76GHz for the turbo mode. These frequencies and modes were selected both for their highest power outputs as well as to cover the

different frequency modes planned for this wireless device. As recommended in Supplement C, Edition 01-01 [3], the stability of the conducted power was determined by repeated SAR measurements at the same location for each of the selected channels. The variability of the SAR thus determined for three repeated measurements over a 60-minute time period was within  $\pm 0.1$  dB ( $\pm 2.5\%$ ).

The highest SAR region for each of the measurement frequencies was identified in the first instance by using a coarser sampling with a step size of 8.0 mm over three overlapping areas for a total scan area of  $8.0 \times 9.6$  cm. The data thus obtained is resolved into a 4 x 4 times larger grid i.e. a grid involving 40 x 28 points by linear interpolation using a 2 mm step size. After thus identifying the region of the highest SAR, the SAR distribution was then measured with a resolution of 2 mm in order to obtain the peak 1 cm<sup>3</sup> or 1-g SAR. The SAR measurements are performed at 4, 6, 8, 10, 12 mm height from the bottom surface of the body-simulant fluid. The SARs thus measured were extrapolated using a fourth-order least-square fit to the measured data to obtain values at 1, 3, 5, 7 and 9 mm height and used to obtain 1-g SARs. The uncertainty analysis of the University of Utah SAR measurement system is given in Appendix B. The combined standard uncertainty is  $\pm 8.3\%$ .

As previously mentioned, two Askey Model WLL220 802.11 a/b antennas are built close to the two edges of the keyboard base for this PC (see Fig. 2). Even though two 802.11a antennas marked "A" and "B" are built into the base of the PC for diversity, only one of the two antennas are active at any given time. For the present measurements, we have determined the SAR distributions for both of the "A" and "B" antennas for the Lap-top and Edge-on positions, respectively. The coarse scans for the various measurements for both the Above-lap Configuration 1 and the Edge-on Configuration 2 (defined in Section I) are shown in Figs. 13-16a-d, respectively. In these figures, the two axes are marked in units of the step size of 8 mm. Also shown in these figures are the respective antenna outlines overlaid on the SAR contours. Given in Tables 3-18 are the SAR distributions for the peak SAR region of volume  $10 \times 10 \times 10$  mm for which the coarse scans are given in Figs. 13-16a-d, respectively.

The SARs are given for xy planes at heights Z of 1, 3, 5, 7, and 9 mm from the bottom of the flat phantom. The individual SAR values for this grid of  $5 \times 5 \times 5$  or 125 points are averaged to obtain peak 1-g SAR values (for a volume of  $1 \text{ cm}^3$ ). The temperature variation of the tissue-simulant fluid measured with a Bailey Instruments Model BAT 8 Temperature Probe over the 80-minute period needed for measurements at the four frequencies was  $23.3 \pm 0.2^\circ \text{C}$ .

As mentioned in Section I, Configuration 1 corresponds to the wireless PC placed on a user's lap – hence, the notebook computer's bottom with antenna "A" or "B" is pressed against the bottom of the planar phantom as shown in Figs. 3a, b, respectively. Similarly, Configuration 2 corresponds to the placement of the right or left edge of the PC at  $90^\circ$  at a distance of 1.5 cm from the bottom of the flat phantom (see Figs. 4a and 4b). This configuration corresponds to a situation when a bystander is standing at a distance of 1.5 cm from the right or the left edges of the PC base. The z-axis scan plots taken at the highest SAR locations for each set of tests are given in Figs. 17-20, respectively. As discussed in Section IV, the SARs at these higher frequencies drop off fairly rapidly with depth in the phantom.

The peak 1-g SARs for the various configurations of the Askey Corporation Model WLL220 Mini PCI Card built into Compal Model BCL50 Notebook Computer (FCC ID#H8NWLL220CL) are summarized in Table 19. All of the measured 1-g SARs are less than the FCC 96-326 guideline of 1.6 W/kg.

## **VII. Comparison of the Data with FCC 96-326 Guidelines**

According to the FCC 96-326 Guideline [1], the peak SAR for any 1-g of tissue should not exceed 1.6 W/kg. For the Askey Corporation Model WLL220 Mini PCI Card built into Compal Model ACY25 Notebook Computer (FCC ID# H8NWLL220C), the measured peak 1-g SARs vary from 0.073 to 0.350 W/kg which are smaller than 1.6 W/kg.

## REFERENCES

1. Federal Communications Commission, "Guidelines for Evaluating the Environmental Effects of Radiofrequency Radiation," FCC 96-326, August 1, 1996.
2. K. Chan, R. F. Cleveland, Jr., and D. L. Means, "Evaluating Compliance With FCC Guidelines for Human Exposure to Radiofrequency Electromagnetic Fields," Supplement C (Edition 97-01) to OET Bulletin 65, December, 1997. Available from Office of Engineering and Technology, Federal Communications Commission, Washington D.C., 20554.
3. Federal Communications Commission "Supplement C Edition 01-01 to OET Bulletin 65 Edition 97-01" June 2001.
4. IEEE Draft Standard P1528, "Recommended Practice for Determining the Peak Spatial-Average Specific Absorption Rate (SAR) in the Human Body Due to Wireless Communication Devices: Experimental Techniques," Draft CBD1.0, April 4, 2002 (IEEE Standards Coordinating Committee 34).
5. O. P. Gandhi and J-Y. Chen, "Electromagnetic Absorption in the Human Head from Experimental 6-GHz Handheld Transceivers," *IEEE Transactions on Electromagnetic Compatibility*, Vol. 39(4), pp. 547-558, 1995.
6. H. Bassen. M. Swicord, and J. Abita, "A Miniature Broadband Electric Field Probe," *Ann. New York Academy of Sciences*, Vol. 247, pp. 481-493, 1974.
7. H. Bassen and T. Babij, "Experimental Techniques and Instrumentation," Chapter 7 in *Biological Effects and Medical Applications of Electromagnetic Energy*, O. P. Gandhi, Editor, Prentice Hall Inc., Englewood Cliffs, NJ, 1990.
8. Q. Yu, O. P. Gandhi, M. Aronsson, and D. Wu, "An Automated SAR Measurement System for Compliance Testing of Personal Wireless Devices," *IEEE Transactions on Electromagnetic Compatibility*, Vol. 41(3), pp. 234-245, August 1999.
9. O. P. Gandhi, *Microwave Engineering and Applications*, Pergamon Press, New York, 1981.
10. T. W. Athey, M. A. Stuchly, and S. S. Stuchly, "Measurement of Radiofrequency Permittivity of Biological Tissues with an Open-Circuited Coaxial Line - Part I," *IEEE Transactions on Microwave Theory and Techniques*, Vol. MTT-30, pp. 82-86, 1982.
11. M. A. Stuchly, T. W. Athey, G. M. Samaras, and G. E. Taylor, "Measurement of Radiofrequency Permittivity of Biological Tissues with an Open-Circuited Coaxial Line - Part II - Experimental Results," *IEEE Transactions on Microwave Theory and Techniques*, Vol. MTT-30, pp. 87-92, 1982.

12. C. L. Pournaropoulos and D. K. Misra, "The Coaxial Aperture Electromagnetic Sensor and Its Application for Material Characterization," *Measurement Science and Technology*, Vol. 8, pp. 1191-1202, 1997.

Table 1. Average conducted RF power outputs measured at various frequencies for the Askey Corporation Model WLL220 Mini PCI Card built into Compal Model BCL50 Notebook Computer for base and turbo modes.

Channel	Frequency GHz	Conducted Output Power (dBm)
	Normal Mode	
1	5.18	16.78
4	5.24	16.93
5	5.26	22.51
8	5.32	22.37
9	5.745	17.08
12	5.805	18.43
Turbo Mode		
1	5.21	16.94
2	5.25	16.93
3	5.29	21.76
4	5.76	19.14
5	5.80	16.03

Table 2. Dielectric parameters for body phantom for the frequency band 5.2 to 5.8 GHz [3].

Frequency GHz	$\epsilon_r$	$\sigma$ S/m	Reference
3.0	52.0	2.73	Ref. 3
5.8	48.2	6.00	Ref. 3
5.25	49.0	5.30	Interpolated
5.3	48.9	5.42	Interpolated
5.4	48.7	5.53	Interpolated
5.6	48.5	5.77	Interpolated
5.7	48.3	5.88	Interpolated

Table 3. **Above-lap position (Configuration 1).** Normal mode at 5.26 GHz. The SARs measured for the Askey WLL220 Mini PCI Card Antenna "A" built into Compal Model BCL50 Notebook Computer.

**1-g SAR = 0.219 W/kg**

**a. At depth of 1 mm**

0.629	0.663	0.659	0.567	0.533
0.598	0.582	0.601	0.515	0.479
0.506	0.513	0.558	0.572	0.510
0.506	0.543	0.542	0.527	0.540
0.466	0.537	0.503	0.421	0.456

**b. At depth of 3 mm**

0.300	0.320	0.301	0.271	0.257
0.294	0.297	0.291	0.270	0.244
0.266	0.276	0.289	0.279	0.263
0.253	0.265	0.274	0.273	0.270
0.248	0.256	0.243	0.232	0.243

**c. At depth of 5 mm**

0.144	0.154	0.134	0.134	0.126
0.144	0.149	0.139	0.136	0.127
0.141	0.144	0.145	0.139	0.136
0.128	0.129	0.140	0.140	0.142
0.134	0.120	0.122	0.126	0.118

**d. At depth of 7 mm**

0.090	0.093	0.080	0.088	0.081
0.090	0.089	0.084	0.076	0.081
0.089	0.085	0.084	0.090	0.085
0.082	0.082	0.088	0.086	0.096
0.085	0.072	0.078	0.075	0.059

**e. At depth of 9 mm**

0.066	0.067	0.060	0.062	0.062
0.070	0.066	0.063	0.053	0.063
0.067	0.069	0.063	0.066	0.065
0.064	0.068	0.067	0.067	0.074
0.064	0.055	0.053	0.050	0.039



Table 4. **Above-lap position (Configuration 1).** Normal mode at 5.805 GHz. The SARs measured for the Askey WLL220 Mini PCI Card Antenna "A" built into Compal Model BCL50 Notebook Computer.

**1-g SAR = 0.136 W/kg**

**a. At depth of 1 mm**

0.187	0.358	0.443	0.281	0.325
0.252	0.315	0.429	0.427	0.363
0.314	0.283	0.212	0.329	0.319
0.301	0.212	0.327	0.258	0.359
0.206	0.317	0.254	0.320	0.348

**b. At depth of 3 mm**

0.165	0.197	0.210	0.163	0.157
0.163	0.176	0.192	0.184	0.166
0.165	0.157	0.148	0.172	0.178
0.164	0.146	0.174	0.158	0.178
0.132	0.156	0.139	0.152	0.148

**c. At depth of 5 mm**

0.124	0.117	0.107	0.090	0.083
0.105	0.099	0.090	0.078	0.078
0.092	0.098	0.097	0.094	0.096
0.097	0.100	0.097	0.096	0.095
0.087	0.078	0.078	0.076	0.049

**d. At depth of 7 mm**

0.086	0.085	0.075	0.055	0.063
0.073	0.064	0.060	0.050	0.054
0.064	0.075	0.066	0.065	0.060
0.070	0.070	0.069	0.065	0.067
0.062	0.049	0.051	0.050	0.011

**e. At depth of 9 mm**

0.074	0.069	0.053	0.050	0.055
0.065	0.053	0.041	0.040	0.050
0.050	0.056	0.059	0.056	0.055
0.055	0.052	0.059	0.055	0.052
0.050	0.034	0.041	0.033	-0.005

Table 5. **Above-lap position (Configuration 1).** Turbo mode at 5.29 GHz. The SARs measured for the Askey WLL220 Mini PCI Card Antenna "A" built into Compal Model BCL50 Notebook Computer.

**1-g SAR = 0.165 W/kg**

**a. At depth of 1 mm**

0.384	0.329	0.316	0.363	0.315
0.417	0.422	0.467	0.334	0.449
0.414	0.441	0.368	0.359	0.341
0.454	0.376	0.437	0.428	0.432
0.349	0.437	0.398	0.448	0.395

**b. At depth of 3 mm**

0.209	0.195	0.182	0.179	0.175
0.206	0.216	0.220	0.186	0.196
0.207	0.216	0.203	0.201	0.185
0.220	0.205	0.209	0.209	0.202
0.193	0.209	0.210	0.220	0.191

**c. At depth of 5 mm**

0.121	0.113	0.107	0.097	0.103
0.106	0.114	0.107	0.106	0.087
0.105	0.107	0.114	0.112	0.103
0.110	0.111	0.106	0.105	0.097
0.108	0.107	0.111	0.108	0.086

**d. At depth of 7 mm**

0.085	0.072	0.072	0.074	0.072
0.071	0.074	0.071	0.070	0.060
0.067	0.069	0.077	0.069	0.069
0.072	0.069	0.073	0.069	0.065
0.070	0.076	0.071	0.067	0.040

**e. At depth of 9 mm**

0.069	0.063	0.055	0.065	0.056
0.058	0.060	0.053	0.051	0.051
0.055	0.053	0.063	0.052	0.053
0.058	0.051	0.053	0.055	0.052
0.055	0.061	0.057	0.051	0.015

Table 6. **Above-lap position (Configuration 1).** Turbo mode at 5.76 GHz. The SARs measured for the Askey WLL220 Mini PCI Card Antenna "A" built into Compal Model BCL50 Notebook Computer.

**1-g SAR = 0.175 W/kg**

**a. At depth of 1 mm**

0.549	0.483	0.423	0.382	0.401
0.481	0.494	0.471	0.472	0.368
0.479	0.467	0.463	0.339	0.445
0.519	0.452	0.509	0.467	0.359
0.563	0.422	0.470	0.427	0.444

**b. At depth of 3 mm**

0.241	0.212	0.198	0.185	0.185
0.230	0.225	0.218	0.217	0.185
0.240	0.228	0.230	0.197	0.210
0.217	0.208	0.219	0.210	0.188
0.222	0.199	0.212	0.194	0.186

**c. At depth of 5 mm**

0.101	0.097	0.098	0.094	0.087
0.118	0.108	0.101	0.103	0.102
0.119	0.118	0.117	0.111	0.100
0.095	0.101	0.091	0.096	0.101
0.089	0.095	0.100	0.088	0.062

**d. At depth of 7 mm**

0.062	0.067	0.067	0.064	0.057
0.081	0.073	0.064	0.068	0.073
0.074	0.082	0.074	0.069	0.063
0.066	0.070	0.057	0.059	0.065
0.065	0.059	0.066	0.053	0.019

**e. At depth of 9 mm**

0.055	0.050	0.052	0.052	0.049
0.055	0.053	0.053	0.050	0.056
0.062	0.071	0.057	0.061	0.046
0.043	0.051	0.046	0.037	0.049
0.052	0.040	0.043	0.031	0.003

Table 7. **Above-lap position (Configuration 1).** Normal mode at 5.26 GHz. The SARs measured for the Askey WLL220 Mini PCI Card Antenna "B" built into Compal Model BCL50 Notebook Computer.

**1-g SAR = 0.292 W/kg**

**a. At depth of 1 mm**

0.589	0.710	0.717	0.797	0.644
0.719	0.723	0.857	0.841	0.793
0.663	0.895	0.870	0.858	0.810
0.639	0.864	0.821	0.836	0.750
0.595	0.727	0.796	0.779	0.722

**b. At depth of 3 mm**

0.302	0.349	0.349	0.377	0.333
0.341	0.369	0.408	0.405	0.385
0.339	0.407	0.426	0.419	0.395
0.330	0.399	0.403	0.409	0.372
0.300	0.347	0.375	0.374	0.333

**c. At depth of 5 mm**

0.146	0.162	0.159	0.175	0.167
0.154	0.178	0.188	0.189	0.182
0.163	0.175	0.199	0.193	0.186
0.162	0.176	0.189	0.186	0.178
0.145	0.163	0.171	0.170	0.147

**d. At depth of 7 mm**

0.079	0.086	0.084	0.102	0.094
0.083	0.096	0.106	0.106	0.101
0.087	0.095	0.108	0.103	0.102
0.088	0.097	0.101	0.096	0.098
0.080	0.096	0.095	0.090	0.078

**e. At depth of 9 mm**

0.058	0.055	0.058	0.072	0.064
0.057	0.067	0.069	0.069	0.060
0.062	0.062	0.071	0.071	0.064
0.062	0.065	0.062	0.068	0.060
0.053	0.069	0.062	0.058	0.039

Table 8. **Above-lap position (Configuration 1).** Normal mode at 5.805 GHz. The SARs measured for the Askey WLL220 Mini PCI Card Antenna "B" built into Compal Model BCL50 Notebook Computer.

**1-g SAR = 0.260 W/kg**

**a. At depth of 1 mm**

0.641	0.777	0.724	0.577	0.610
0.676	0.621	0.741	0.703	0.615
0.631	0.687	0.736	0.762	0.635
0.721	0.626	0.811	0.745	0.655
0.670	0.754	0.739	0.690	0.660

**b. At depth of 3 mm**

0.302	0.332	0.323	0.289	0.297
0.323	0.321	0.338	0.320	0.300
0.311	0.326	0.354	0.348	0.304
0.318	0.318	0.356	0.333	0.309
0.303	0.336	0.335	0.316	0.290

**c. At depth of 5 mm**

0.140	0.138	0.146	0.142	0.146
0.154	0.158	0.149	0.147	0.138
0.140	0.151	0.160	0.153	0.139
0.139	0.152	0.151	0.146	0.142
0.132	0.148	0.146	0.133	0.119

**d. At depth of 7 mm**

0.080	0.084	0.096	0.088	0.092
0.096	0.087	0.086	0.092	0.074
0.071	0.089	0.085	0.089	0.079
0.086	0.082	0.088	0.086	0.082
0.080	0.090	0.082	0.067	0.061

**e. At depth of 9 mm**

0.046	0.059	0.077	0.080	0.072
0.078	0.064	0.064	0.061	0.052
0.058	0.064	0.062	0.068	0.062
0.061	0.065	0.056	0.059	0.056
0.070	0.062	0.052	0.044	0.030

Table 9. **Above-lap position (Configuration 1).** Turbo mode at 5.29 GHz. The SARs measured for the Askey WLL220 Mini PCI Card Antenna "B" built into Compal Model BCL50 Notebook Computer.

**1-g SAR = 0.261 W/kg**

**a. At depth of 1 mm**

0.654	0.605	0.621	0.644	0.620
0.705	0.633	0.713	0.713	0.633
0.675	0.717	0.745	0.709	0.663
0.637	0.786	0.679	0.780	0.621
0.609	0.654	0.742	0.692	0.606

**b. At depth of 3 mm**

0.314	0.310	0.311	0.308	0.296
0.341	0.345	0.350	0.340	0.304
0.340	0.368	0.380	0.353	0.318
0.328	0.374	0.351	0.366	0.306
0.303	0.326	0.343	0.329	0.284

**c. At depth of 5 mm**

0.146	0.153	0.152	0.146	0.139
0.167	0.175	0.170	0.159	0.141
0.160	0.179	0.183	0.165	0.148
0.158	0.174	0.172	0.163	0.146
0.143	0.154	0.152	0.146	0.123

**d. At depth of 7 mm**

0.083	0.086	0.087	0.088	0.083
0.104	0.093	0.099	0.090	0.079
0.085	0.095	0.097	0.086	0.083
0.084	0.098	0.093	0.087	0.082
0.079	0.083	0.086	0.076	0.058

**e. At depth of 9 mm**

0.056	0.060	0.057	0.067	0.060
0.071	0.065	0.064	0.057	0.055
0.060	0.065	0.070	0.054	0.054
0.062	0.061	0.064	0.054	0.053
0.057	0.057	0.060	0.048	0.023

Table 10. **Above-lap position (Configuration 1).** Turbo mode at 5.76 GHz. The SARs measured for the Askey WLL220 Mini PCI Card Antenna "B" built into Compal Model BCL50 Notebook Computer.

**1-g SAR = 0.350 W/kg**

**a. At depth of 1 mm**

0.863	0.909	0.874	0.770	0.824
0.902	0.998	0.972	0.893	0.936
0.863	0.935	0.979	0.945	1.006
0.817	1.032	0.914	1.060	0.914
0.696	0.774	0.863	0.905	0.885

**b. At depth of 3 mm**

0.403	0.420	0.422	0.402	0.384
0.427	0.451	0.461	0.440	0.431
0.409	0.450	0.464	0.477	0.465
0.393	0.457	0.457	0.487	0.453
0.357	0.402	0.434	0.444	0.412

**c. At depth of 5 mm**

0.183	0.189	0.196	0.203	0.182
0.203	0.204	0.211	0.214	0.198
0.192	0.219	0.220	0.231	0.212
0.189	0.201	0.222	0.223	0.213
0.180	0.207	0.209	0.210	0.182

**d. At depth of 7 mm**

0.107	0.111	0.115	0.117	0.117
0.124	0.129	0.121	0.126	0.120
0.117	0.137	0.137	0.130	0.127
0.115	0.128	0.129	0.137	0.118
0.112	0.125	0.118	0.116	0.100

**e. At depth of 9 mm**

0.080	0.083	0.096	0.087	0.089
0.085	0.096	0.089	0.090	0.083
0.089	0.095	0.104	0.101	0.090
0.083	0.099	0.099	0.095	0.087
0.099	0.092	0.090	0.081	0.071

Table 11. **Edge-on position (Configuration 2).** Normal mode at 5.26 GHz. The SARs measured for the Askey WLL220 Mini PCI Card Antenna "A" built into Compal Model BCL50 Notebook Computer.

**1-g SAR = 0.249 W/kg**

**a. At depth of 1 mm**

0.626	0.666	0.719	0.707	0.566
0.574	0.594	0.704	0.657	0.616
0.609	0.702	0.699	0.750	0.682
0.614	0.679	0.755	0.677	0.675
0.558	0.596	0.702	0.648	0.687

**b. At depth of 3 mm**

0.293	0.312	0.324	0.315	0.273
0.288	0.303	0.332	0.318	0.296
0.286	0.325	0.344	0.346	0.319
0.291	0.329	0.348	0.335	0.315
0.263	0.295	0.322	0.307	0.300

**c. At depth of 5 mm**

0.134	0.145	0.143	0.133	0.131
0.141	0.146	0.151	0.149	0.138
0.130	0.148	0.158	0.159	0.148
0.137	0.154	0.151	0.155	0.146
0.124	0.141	0.142	0.138	0.119

**d. At depth of 7 mm**

0.079	0.087	0.085	0.076	0.079
0.078	0.079	0.085	0.084	0.079
0.075	0.088	0.083	0.095	0.088
0.083	0.085	0.082	0.080	0.087
0.076	0.077	0.078	0.074	0.058

**e. At depth of 9 mm**

0.062	0.061	0.060	0.060	0.055
0.046	0.053	0.058	0.055	0.053
0.055	0.064	0.061	0.060	0.060
0.063	0.053	0.060	0.051	0.057
0.051	0.044	0.046	0.044	0.028



Table 12. **Edge-on position (Configuration 2).** Normal mode at 5.805 GHz. The SARs measured for the Askey WLL220 Mini PCI Card Antenna "A" built into Compal Model BCL50 Notebook Computer.

**1-g SAR = 0.154 W/kg**

**a. At depth of 1 mm**

0.321	0.355	0.286	0.434	0.366
0.307	0.310	0.299	0.286	0.294
0.353	0.297	0.302	0.321	0.399
0.284	0.242	0.363	0.391	0.391
0.249	0.360	0.167	0.277	0.238

**b. At depth of 3 mm**

0.181	0.187	0.180	0.198	0.203
0.180	0.181	0.189	0.182	0.182
0.186	0.193	0.187	0.185	0.207
0.171	0.152	0.186	0.201	0.193
0.153	0.178	0.140	0.159	0.158

**c. At depth of 5 mm**

0.112	0.109	0.115	0.114	0.118
0.118	0.116	0.126	0.122	0.124
0.111	0.125	0.121	0.114	0.118
0.108	0.105	0.106	0.110	0.101
0.099	0.102	0.106	0.093	0.102

**d. At depth of 7 mm**

0.088	0.084	0.083	0.100	0.086
0.092	0.091	0.096	0.092	0.102
0.092	0.091	0.090	0.089	0.092
0.081	0.085	0.081	0.079	0.072
0.076	0.081	0.079	0.065	0.065

**e. At depth of 9 mm**

0.083	0.071	0.075	0.081	0.080
0.074	0.077	0.087	0.076	0.095
0.090	0.090	0.081	0.090	0.090
0.071	0.075	0.071	0.068	0.062
0.075	0.065	0.071	0.061	0.044

Table 13. **Edge-on position (Configuration 2).** Turbo mode at 5.29 GHz. The SARs measured for the Askey WLL220 Mini PCI Card Antenna "A" built into Compal Model BCL50 Notebook Computer.

**1-g SAR = 0.201 W/kg**

**a. At depth of 1 mm**

0.438	0.440	0.403	0.476	0.426
0.467	0.548	0.518	0.562	0.513
0.608	0.557	0.556	0.570	0.446
0.396	0.527	0.534	0.545	0.559
0.447	0.514	0.547	0.463	0.404

**b. At depth of 3 mm**

0.220	0.233	0.238	0.245	0.219
0.233	0.254	0.251	0.259	0.243
0.253	0.263	0.272	0.273	0.238
0.218	0.260	0.273	0.273	0.273
0.220	0.245	0.263	0.250	0.221

**c. At depth of 5 mm**

0.116	0.125	0.138	0.129	0.116
0.118	0.123	0.122	0.123	0.117
0.106	0.124	0.131	0.135	0.126
0.118	0.131	0.139	0.134	0.134
0.112	0.120	0.125	0.130	0.114

**d. At depth of 7 mm**

0.078	0.082	0.087	0.084	0.076
0.076	0.081	0.076	0.081	0.073
0.070	0.079	0.078	0.088	0.076
0.073	0.084	0.084	0.079	0.083
0.075	0.077	0.075	0.074	0.058

**e. At depth of 9 mm**

0.060	0.067	0.070	0.067	0.057
0.058	0.053	0.059	0.059	0.050
0.053	0.062	0.060	0.059	0.055
0.060	0.064	0.059	0.060	0.066
0.059	0.055	0.050	0.051	0.030

Table 14. **Edge-on position (Configuration 2).** Turbo mode at 5.76 GHz. The SARs measured for the Askey WLL220 Mini PCI Card Antenna "A" built into Compal Model BCL50 Notebook Computer.

**1-g SAR = 0.190 W/kg**

**a. At depth of 1 mm**

0.498	0.580	0.490	0.515	0.398
0.569	0.515	0.449	0.555	0.392
0.409	0.562	0.548	0.522	0.424
0.377	0.385	0.444	0.534	0.505
0.420	0.487	0.541	0.450	0.466

**b. At depth of 3 mm**

0.252	0.264	0.236	0.239	0.220
0.247	0.235	0.229	0.243	0.201
0.235	0.267	0.261	0.246	0.219
0.198	0.211	0.230	0.251	0.234
0.213	0.232	0.239	0.213	0.211

**c. At depth of 5 mm**

0.125	0.123	0.113	0.111	0.118
0.110	0.104	0.109	0.103	0.105
0.131	0.124	0.123	0.118	0.110
0.104	0.109	0.117	0.119	0.104
0.112	0.112	0.095	0.095	0.101

**d. At depth of 7 mm**

0.074	0.079	0.071	0.071	0.071
0.073	0.064	0.060	0.063	0.068
0.080	0.076	0.077	0.075	0.065
0.064	0.063	0.070	0.075	0.062
0.073	0.071	0.050	0.053	0.065

**e. At depth of 9 mm**

0.056	0.055	0.061	0.055	0.059
0.050	0.052	0.053	0.053	0.056
0.060	0.066	0.068	0.053	0.052
0.050	0.056	0.055	0.058	0.052
0.052	0.053	0.039	0.042	0.033

Table 15. **Above-lap position (Configuration 1).** Normal mode at 5.26 GHz. The SARs measured for the Askey WLL220 Mini PCI Card Antenna "B" built into Compal Model BCL50 Notebook Computer.

**1-g SAR = 0.073W/kg**

**a. At depth of 1 mm**

0.103	0.124	0.181	0.188	0.145
0.154	0.145	0.120	0.176	0.055
0.159	0.169	0.119	0.141	0.146
0.083	0.177	0.200	0.150	0.081
0.131	0.235	0.100	0.148	0.071

**b. At depth of 3 mm**

0.082	0.089	0.101	0.102	0.086
0.092	0.086	0.089	0.093	0.065
0.089	0.087	0.076	0.093	0.096
0.082	0.106	0.101	0.085	0.062
0.089	0.102	0.081	0.074	0.057

**c. At depth of 5 mm**

0.067	0.063	0.061	0.063	0.058
0.061	0.054	0.061	0.059	0.057
0.056	0.048	0.057	0.061	0.063
0.069	0.068	0.057	0.051	0.046
0.058	0.052	0.057	0.045	0.040

**d. At depth of 7 mm**

0.054	0.049	0.047	0.051	0.051
0.046	0.041	0.042	0.046	0.042
0.042	0.035	0.051	0.043	0.047
0.055	0.052	0.045	0.038	0.034
0.041	0.045	0.037	0.036	0.027

**e. At depth of 9 mm**

0.042	0.049	0.044	0.043	0.053
0.037	0.039	0.040	0.030	0.035
0.029	0.031	0.041	0.039	0.047
0.053	0.048	0.042	0.035	0.027
0.040	0.044	0.032	0.023	0.025

Table 16. **Edge-on position (Configuration 2).** Normal mode at 5.805 GHz. The SARs measured for the Askey WLL220 Mini PCI Card Antenna "B" built into Compal Model BCL50 Notebook Computer.

**1-g SAR = 0.180 W/kg**

**a. At depth of 1 mm**

0.369	0.398	0.430	0.426	0.383
0.385	0.378	0.508	0.473	0.434
0.386	0.367	0.438	0.395	0.304
0.463	0.467	0.437	0.415	0.353
0.388	0.343	0.324	0.378	0.416

**b. At depth of 3 mm**

0.202	0.229	0.228	0.219	0.208
0.217	0.223	0.247	0.232	0.217
0.204	0.208	0.224	0.211	0.187
0.224	0.222	0.216	0.214	0.195
0.201	0.195	0.189	0.201	0.189

**c. At depth of 5 mm**

0.123	0.140	0.127	0.122	0.126
0.134	0.137	0.133	0.125	0.115
0.117	0.122	0.121	0.123	0.120
0.118	0.115	0.118	0.118	0.118
0.110	0.117	0.122	0.115	0.090

**d. At depth of 7 mm**

0.097	0.101	0.090	0.092	0.096
0.104	0.098	0.102	0.094	0.084
0.087	0.086	0.084	0.090	0.089
0.085	0.084	0.090	0.085	0.089
0.080	0.084	0.092	0.082	0.061

**e. At depth of 9 mm**

0.086	0.084	0.081	0.083	0.077
0.093	0.086	0.089	0.076	0.077
0.073	0.073	0.071	0.070	0.080
0.065	0.068	0.081	0.075	0.074
0.074	0.072	0.072	0.062	0.044

Table 17. **Edge-on position (Configuration 2).** Turbo mode at 5.29 GHz. The SARs measured for the Askey WLL220 Mini PCI Card Antenna "B" built into Compal Model BCL50 Notebook Computer.

**1-g SAR = 0.089 W/kg**

**a. At depth of 1 mm**

0.134	0.163	0.118	0.162	0.155
0.089	0.123	0.232	0.193	0.100
0.182	0.173	0.168	0.156	0.131
0.116	0.163	0.188	0.140	0.193
0.163	0.178	0.209	0.155	0.102

**b. At depth of 3 mm**

0.089	0.102	0.098	0.103	0.094
0.081	0.092	0.117	0.109	0.093
0.109	0.109	0.106	0.107	0.096
0.089	0.109	0.114	0.099	0.097
0.099	0.103	0.108	0.092	0.078

**c. At depth of 5 mm**

0.072	0.072	0.083	0.074	0.065
0.066	0.077	0.071	0.071	0.082
0.080	0.078	0.076	0.077	0.073
0.070	0.081	0.078	0.071	0.061
0.070	0.066	0.070	0.066	0.057

**d. At depth of 7 mm**

0.068	0.062	0.072	0.062	0.057
0.054	0.069	0.060	0.060	0.071
0.071	0.065	0.064	0.061	0.063
0.061	0.069	0.064	0.056	0.055
0.059	0.053	0.061	0.057	0.041

**e. At depth of 9 mm**

0.062	0.059	0.064	0.057	0.058
0.053	0.058	0.053	0.053	0.065
0.061	0.058	0.058	0.055	0.063
0.058	0.060	0.055	0.051	0.048
0.051	0.048	0.050	0.048	0.030

Table 18. **Above-lap position (Configuration 1).** Turbo mode at 5.76 GHz. The SARs measured for the Askey WLL220 Mini PCI Card Antenna "B" built into Compal Model BCL50 Notebook Computer.

**1-g SAR = 0.166 W/kg**

**a. At depth of 1 mm**

0.425	0.390	0.400	0.423	0.371
0.282	0.469	0.413	0.393	0.396
0.382	0.375	0.420	0.460	0.376
0.409	0.422	0.402	0.433	0.367
0.416	0.337	0.391	0.358	0.273

**b. At depth of 3 mm**

0.198	0.194	0.197	0.208	0.185
0.174	0.226	0.211	0.212	0.199
0.204	0.206	0.218	0.227	0.190
0.203	0.207	0.206	0.207	0.179
0.202	0.171	0.180	0.184	0.156

**c. At depth of 5 mm**

0.106	0.106	0.109	0.114	0.099
0.112	0.116	0.116	0.121	0.113
0.122	0.120	0.124	0.118	0.102
0.104	0.108	0.107	0.103	0.097
0.101	0.089	0.091	0.094	0.077

**d. At depth of 7 mm**

0.085	0.076	0.084	0.083	0.074
0.082	0.083	0.083	0.085	0.089
0.095	0.087	0.090	0.080	0.075
0.070	0.073	0.067	0.069	0.074
0.063	0.059	0.067	0.057	0.030

**e. At depth of 9 mm**

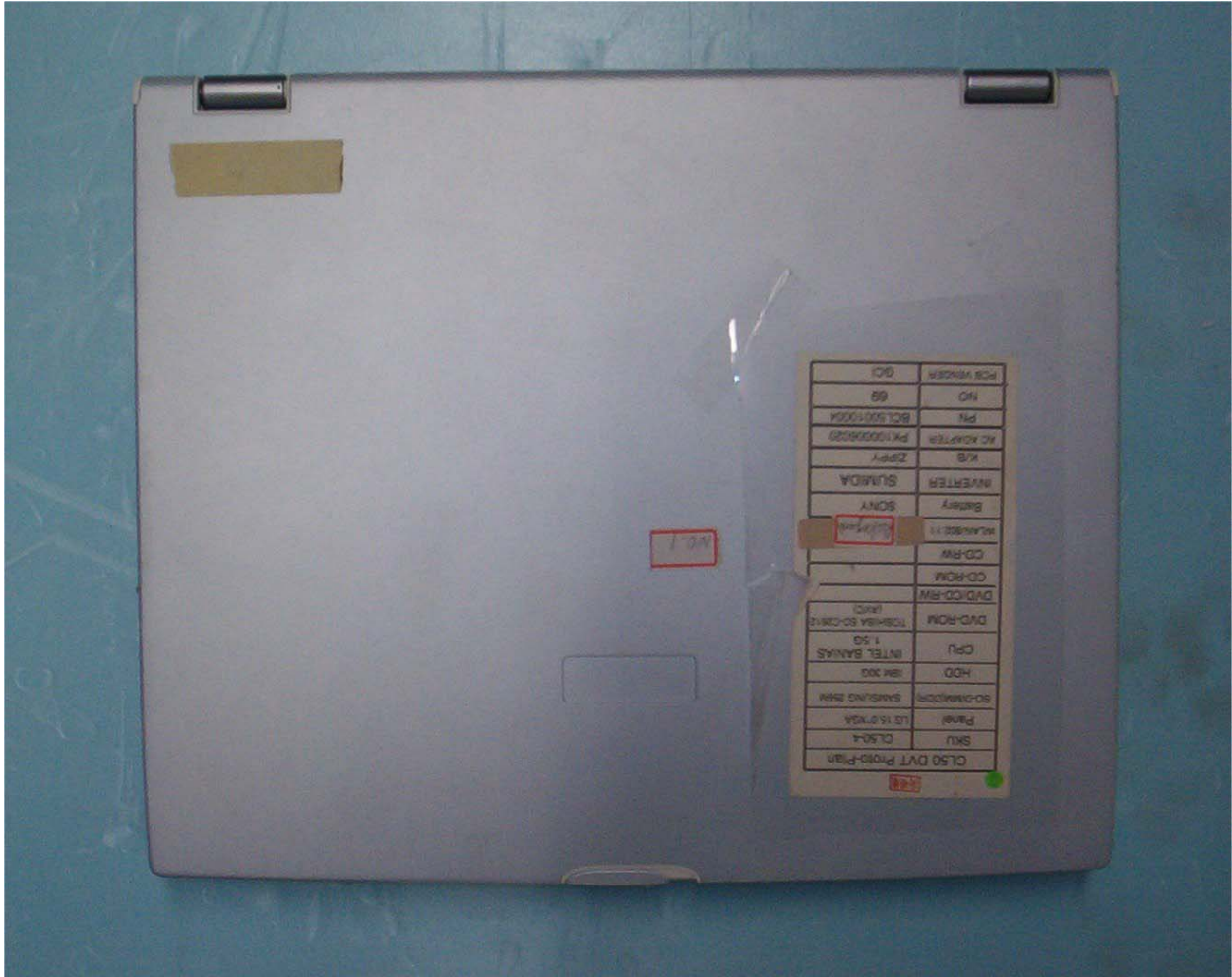
0.074	0.056	0.068	0.059	0.070
0.067	0.074	0.066	0.071	0.080
0.076	0.077	0.071	0.065	0.068
0.059	0.049	0.047	0.053	0.062
0.040	0.047	0.049	0.044	0.010

Table 19. The peak 1-g SARs measured for the Askey Computer Corporation Model WLL220 Mini PCI Card built into Compal Model BCL50 Notebook Computer (FCC ID# H8NWLL220CL).

**1-g SAR in W/kg**

PC position relative to the flat phantom	Spacing to the bottom of the phantom	Antenna	5.26 GHz normal mode	5.805 GHz normal mode	5.29 GHz turbo mode	5.76 GHz turbo mode
<b>Configuration 1 – "Above-lap" position;</b> bottom of PC pressed against bottom of the flat phantom (see Figs. 3a,b)	0 cm	"A"	0.219	0.136	0.165	0.175
		"B"	0.292	0.260	0.261	0.350
<b>Configuration 2 – "Edge-on" placement;</b> right or left edge of the PC at 90° and at a distance of 1.5 cm from the base of the phantom (see Figs. 4a, 4b)	1.5 cm	"A"	0.249	0.154	0.201	0.190
		"B"	0.073	0.180	0.089	0.166





a. Top cover closed.

Fig. 1. Photograph of the Compal Model BCL50 Notebook Computer with built-in Askey Corporation Model WLL220 Mini PCI Card.



b. View from bottom side of the laptop computer.

Fig. 1. Photograph of the Compal Model BCL50 Notebook Computer with built-in Askey Corporation Model WLL220 Mini PCI Card.



c. Top cover with screen open.

Fig. 1. Photograph of the Compaq Model BCL50 Notebook Computer with built-in Askey Corporation Model WLL220 Mini PCI Card.

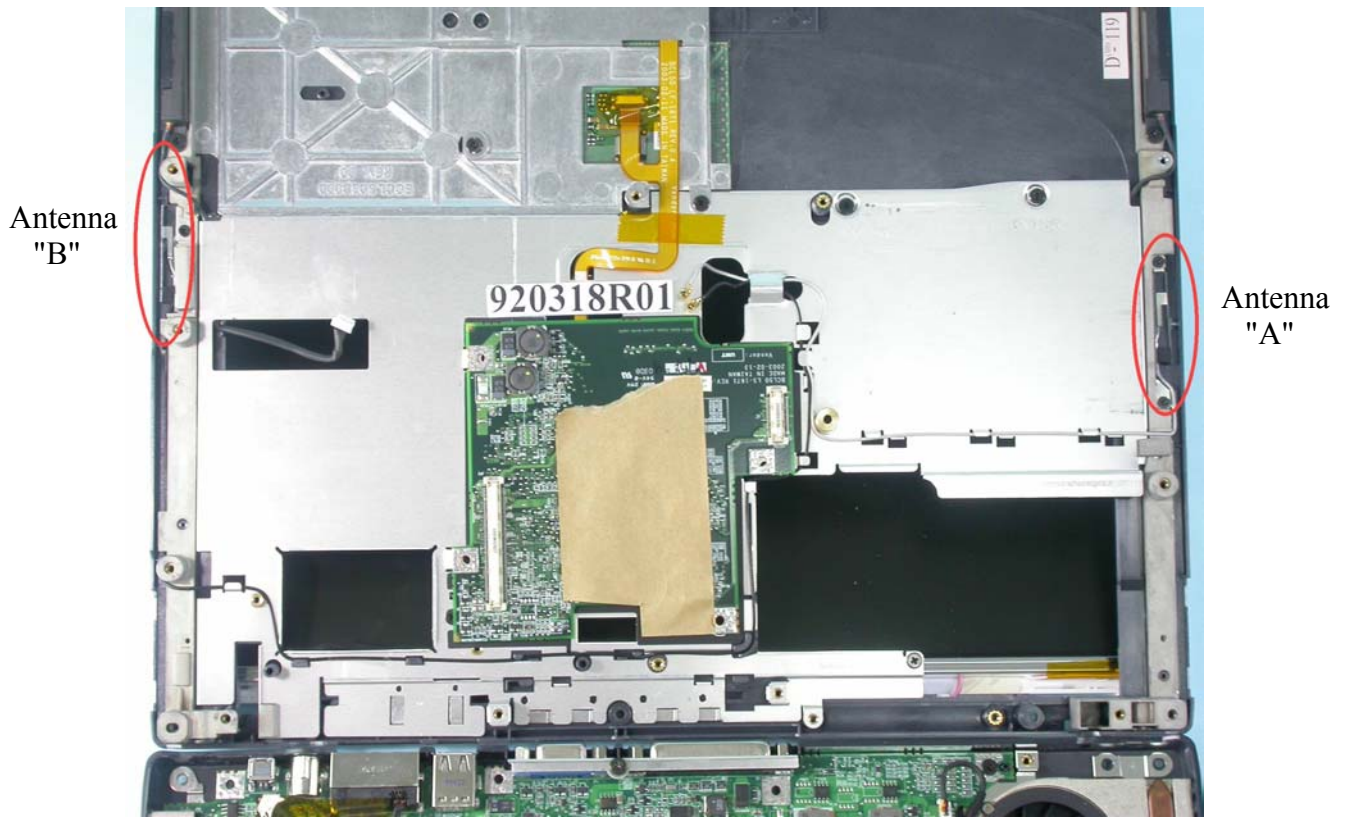
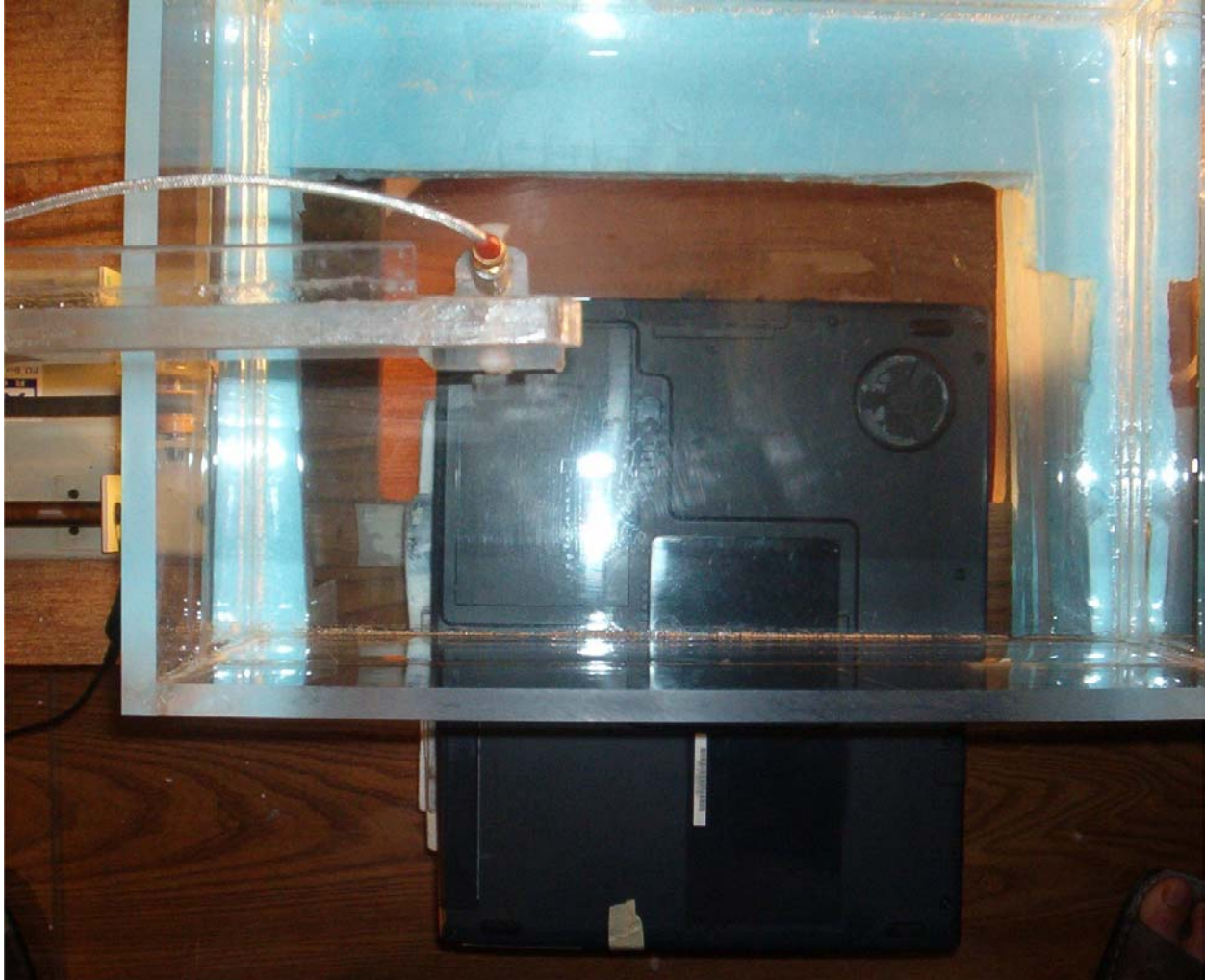
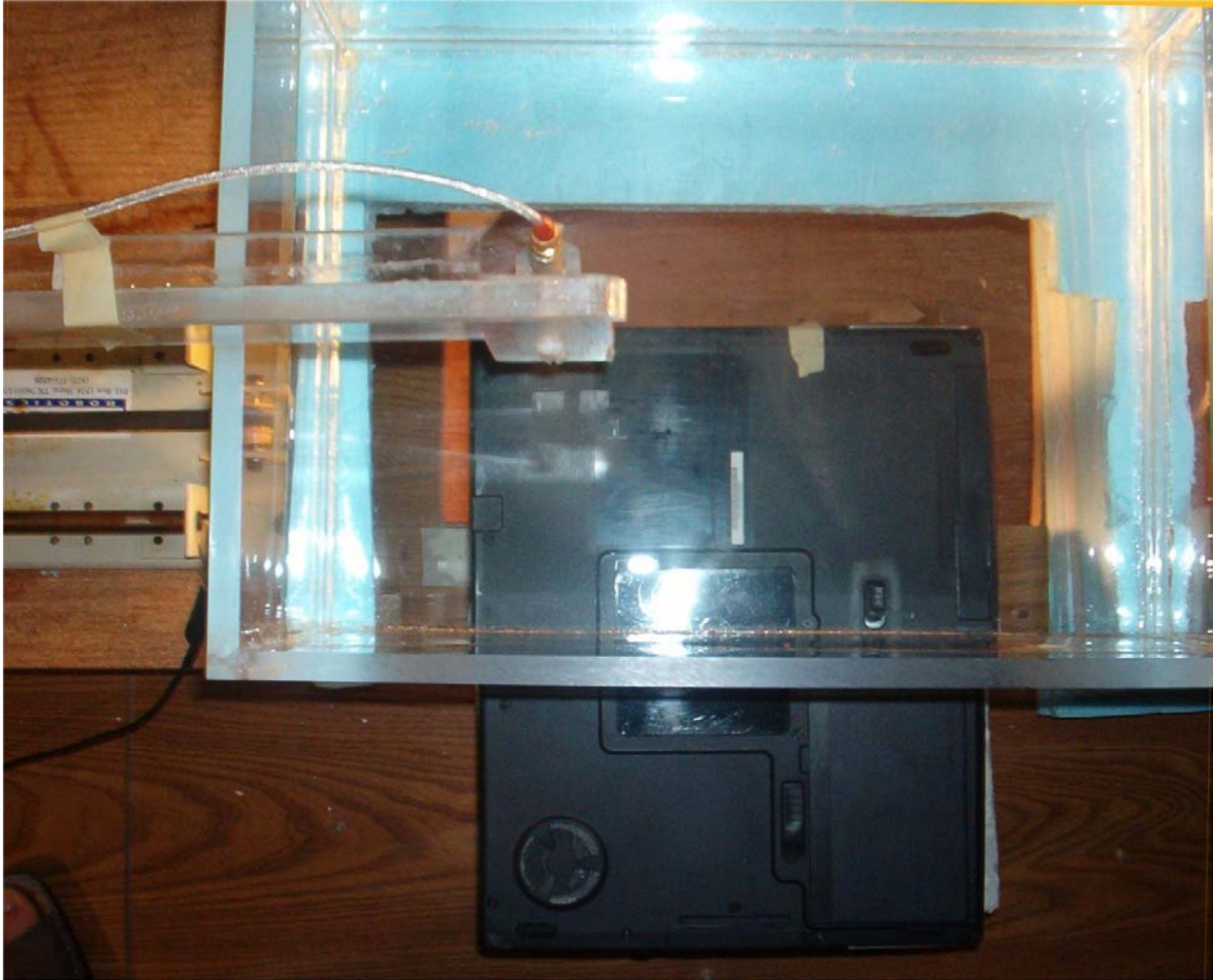


Fig. 2. Photograph of the base of the Compal Model BCL50 Notebook Computer showing the relative locations of Askey Model WLL220 802.11a Wireless Antennas marked as "A" and "B" antennas.



a. The right half of the PC with antenna "A" pressed against the planar phantom.

Fig. 3. Photograph of the bottom of the Model BCL50 Notebook Computer with built-in Askey Model WLL220 Mini PCI Card 802.11a Wireless Antennas pressed against the base of the planar phantom. This is **Configuration 1 – Laptop position** for SAR testing.



b. The left half of the PC with antenna "B" pressed against the planar phantom.

Fig. 3. Photograph of the bottom of the Model BCL50 Notebook Computer with built-in Askey Model WLL220 Mini PCI Card 802.11a Wireless Antennas pressed against the base of the planar phantom. This is **Configuration 1 – Laptop position** for SAR testing.



- a. The right edge with antenna "A" at a distance of 1.5 cm from the bottom of the planar phantom.

Fig. 4. Photograph of the Model BCL50 Notebook Computer with edge of the PC at 90° and placed at a distance of 1.5 cm from the base of the planar phantom. This is **Configuration 2** for SAR testing and represents the case of a bystander at a distance of 1.5 cm from the side of the laptop computer.



- b. The left edge with antenna "B" at a distance of 1.5 cm the bottom of the planar phantom.

Fig. 4. Photograph of the Model BCL50 Notebook Computer with edge of the PC at  $90^\circ$  and placed at a distance of 1.5 cm from the base of the planar phantom. This is **Configuration 2** for SAR testing and represents the case of a bystander at a distance of 1.5 cm from the side of the laptop computer.



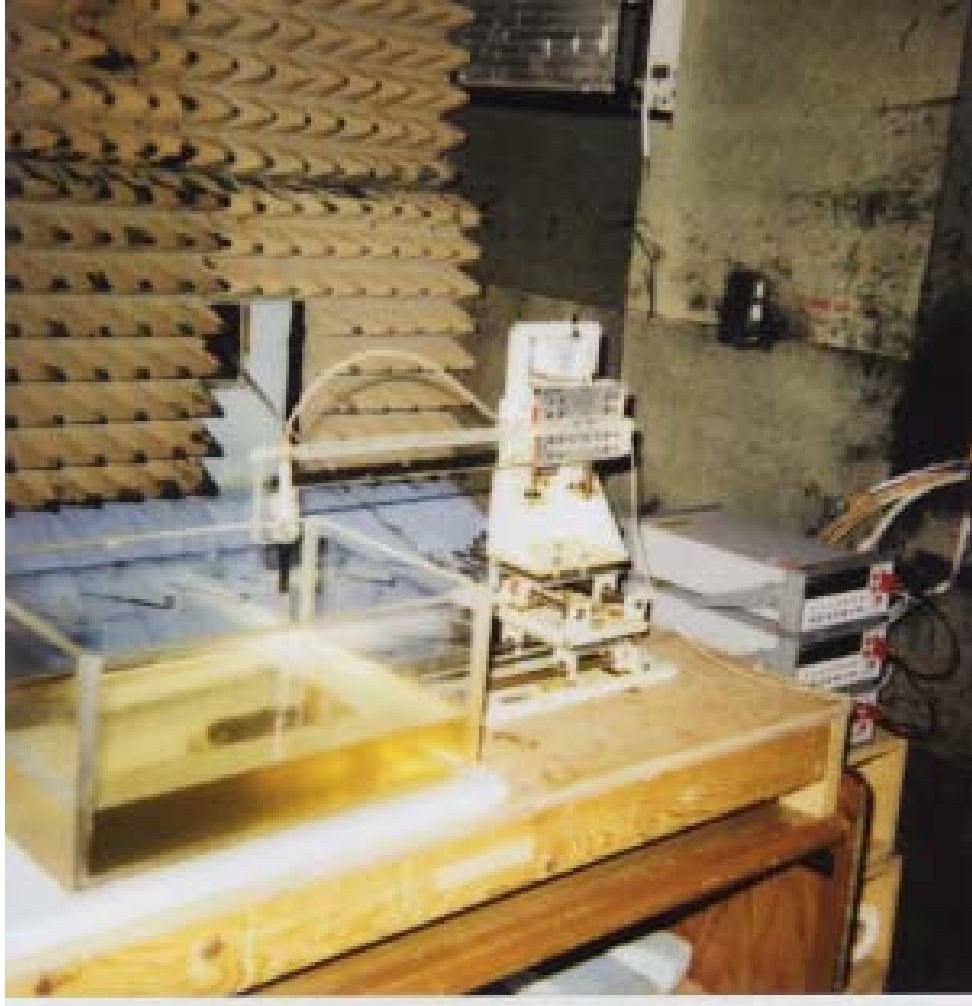


Fig. 5. Photograph of the three-dimensional stepper-motor-controlled SAR measurement system using a planar phantom (see Figs. 3 and 4 for a detailed examination of the placement of the Model BCL50 Notebook Computer with Askey Model WLL220 802.11a Wireless Antennas relative to this phantom).

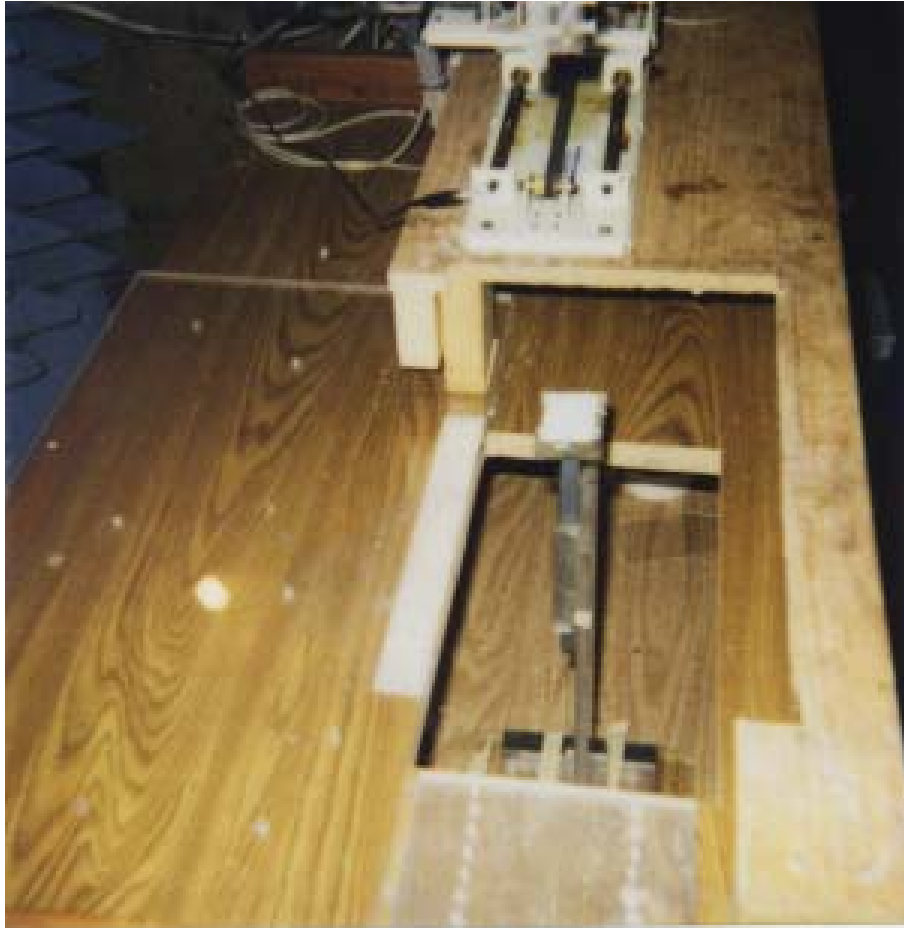


Fig. 6. The plastic holder used to support the portable PC with the Askey WLL220 Mini PCI Card (shown in Figs. 1,2).

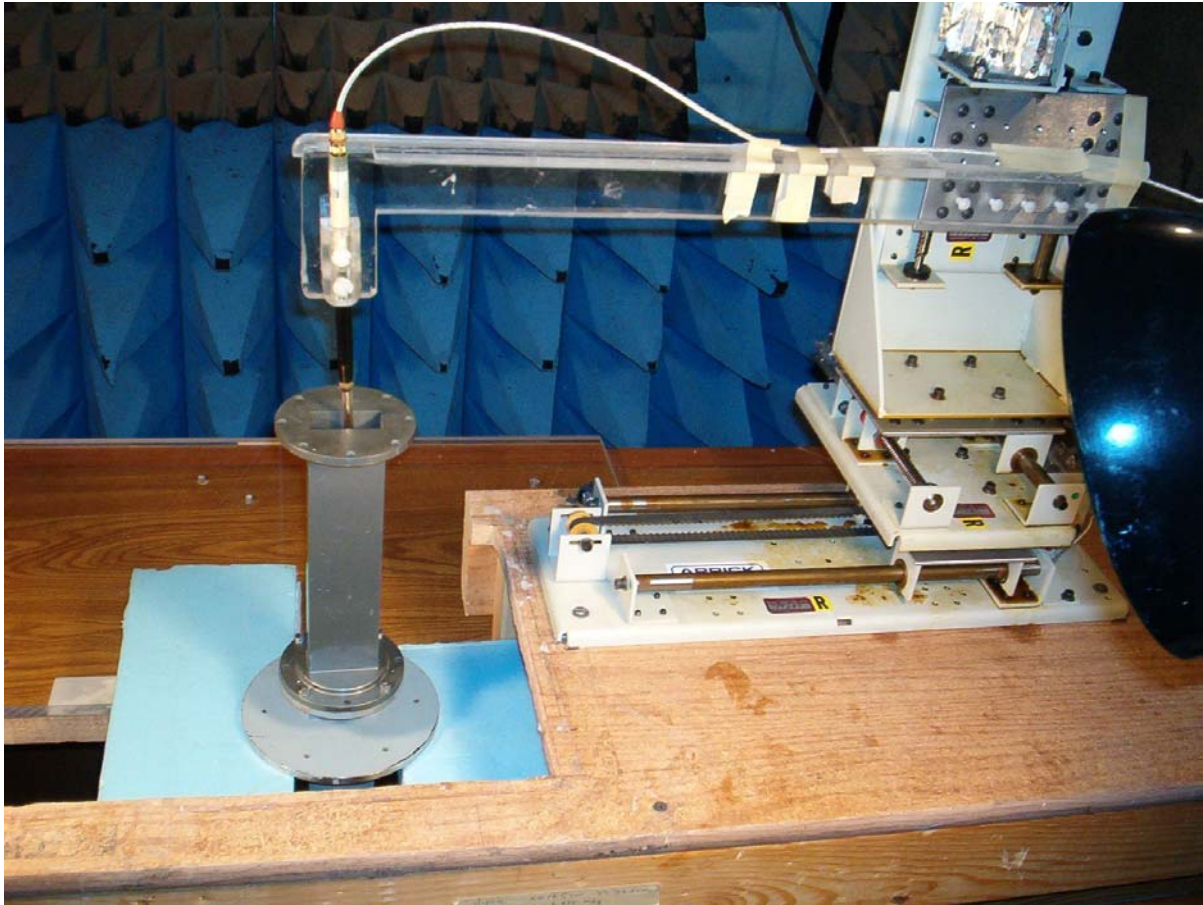


Fig. 7a. A photograph of the waveguide setup used for calibration of the Narda Model 8021 E-field probe in the frequency band 5.2-5.8 GHz.

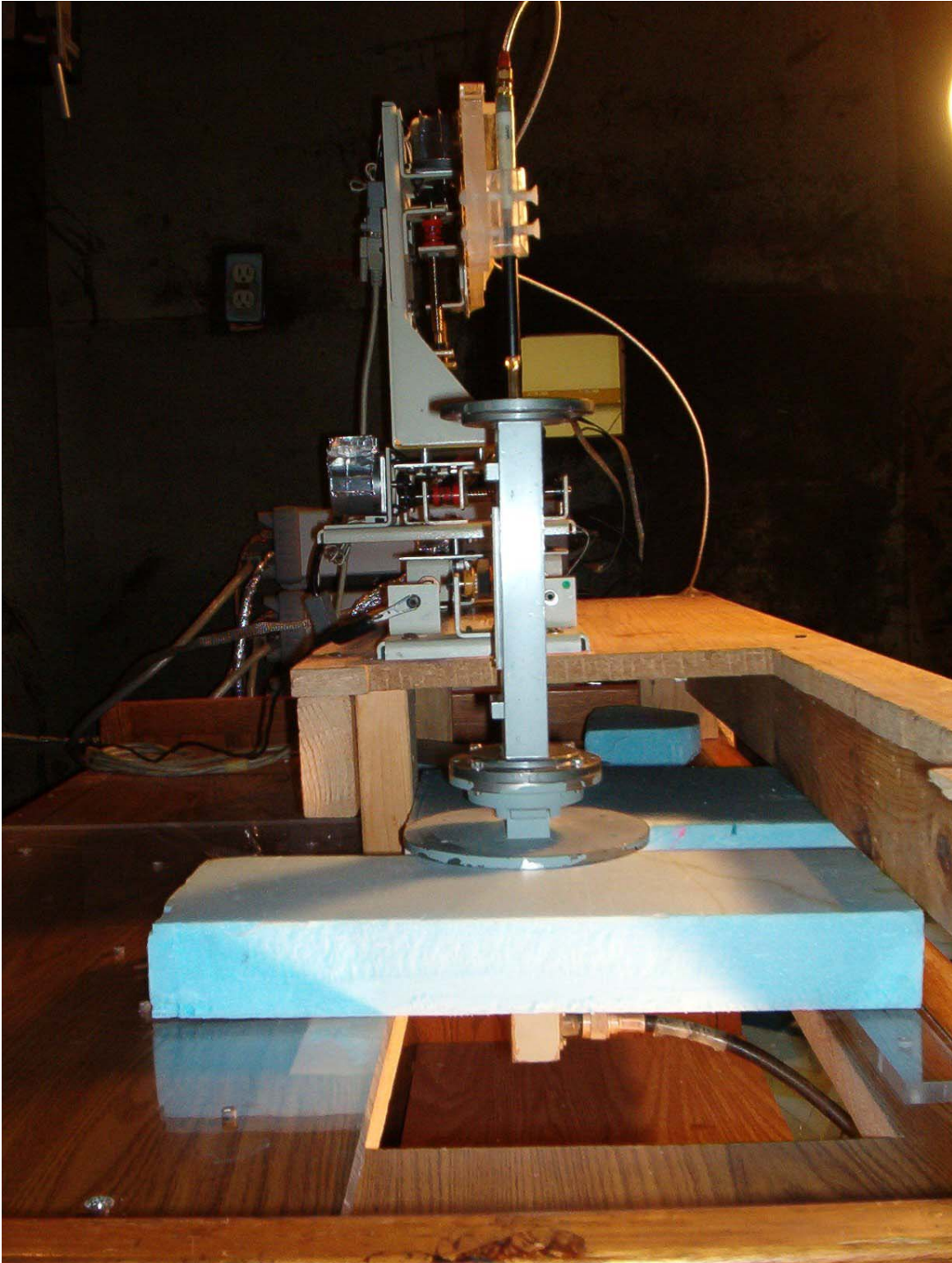


Fig. 7b. Photograph of the waveguide setup showing also the coax to waveguide coupler at the bottom used to feed power to the vertical waveguide containing the tissue-simulant fluid.



Fig. 8. Photograph of the Narda Model 8021 Broadband Electric Field Probe used for SAR measurements.

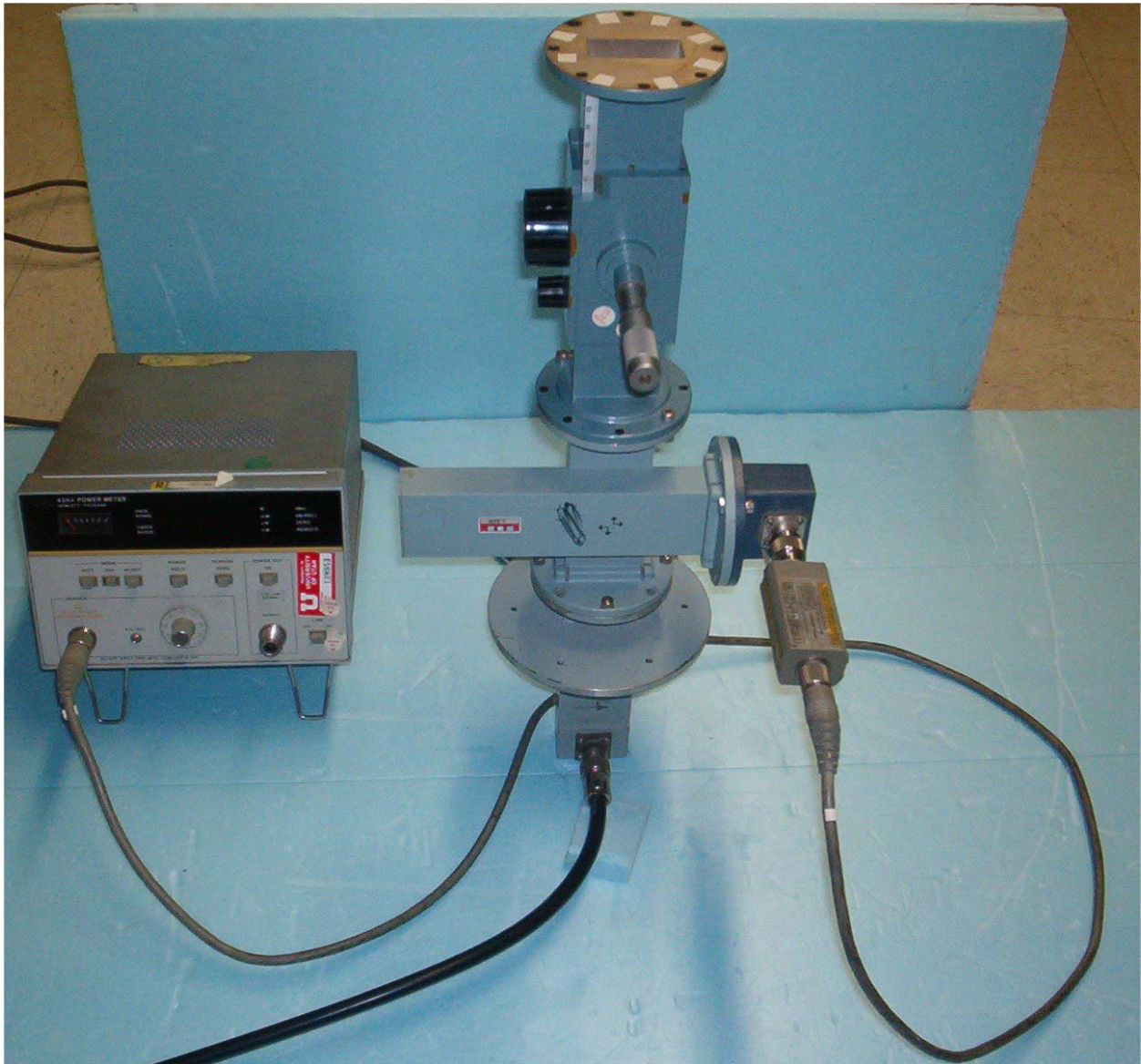
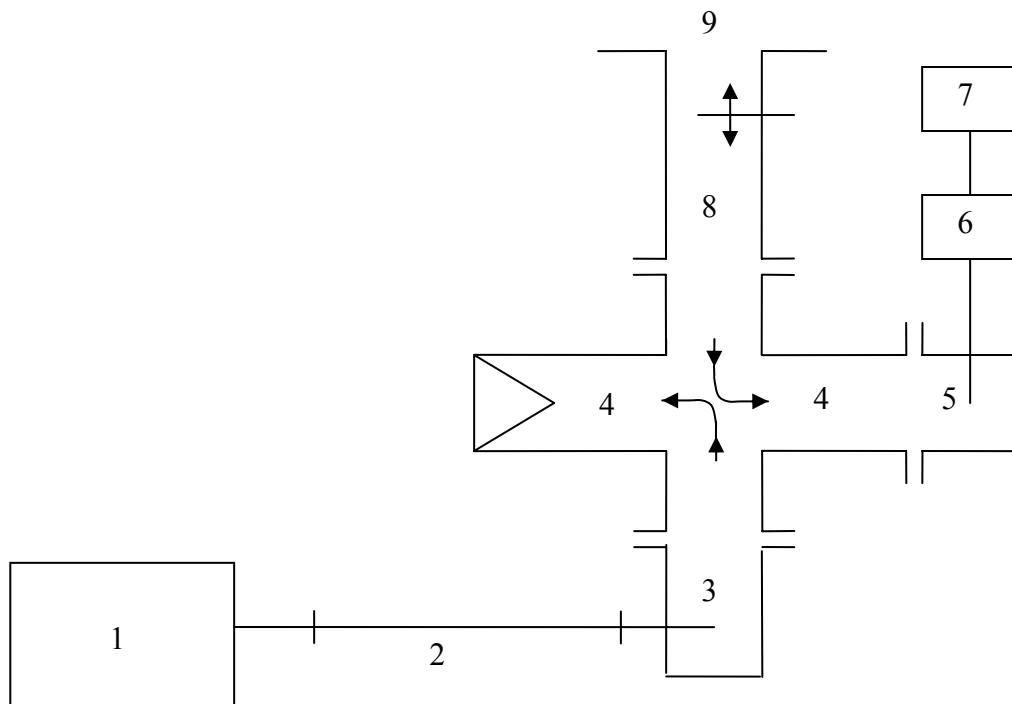
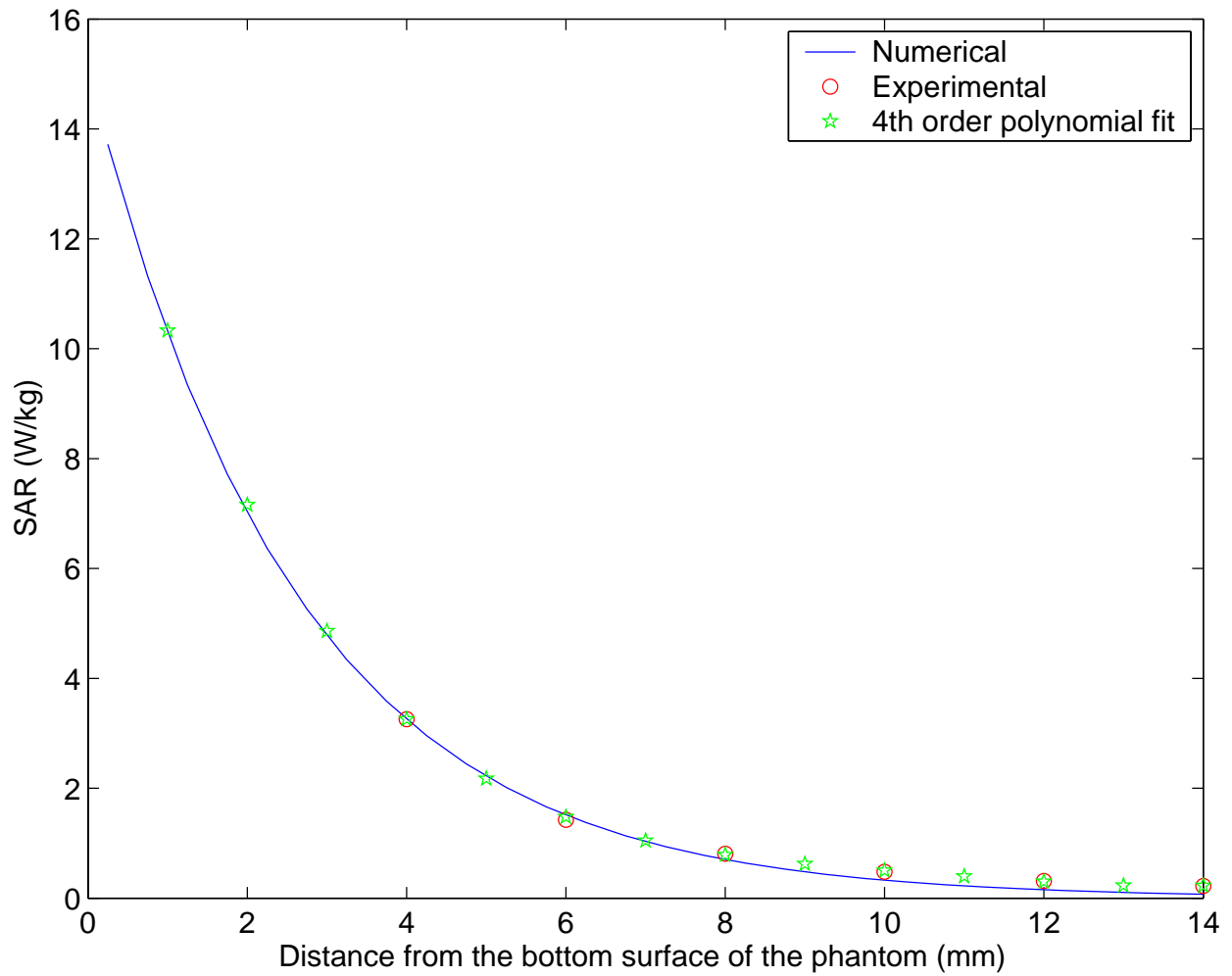


Fig. 9. Photograph of the rectangular waveguide radiator used for system verification. Also seen is the Narda Model 22CI movable slide screw tuner used to match the input power at 5.25 or 5.8 GHz to the planar phantom.



1. Hewlett Packard (HP) Model 83620A Synthesized Sweeper (10 MHz-20 GHz).
2. Coaxial line.
3. Coaxial to waveguide adapter.
4. 20 dB crossguide coupler (may be reversed to measure incident power).
5. HP Model G281A coaxial to waveguide adapter
6. HP Model 8482A power sensor.
7. HP Model 436A power meter.
8. Narda Microline<sup>®</sup> Slide Screw Tuner Model 22CI.
9. Radiating open end of the waveguide.

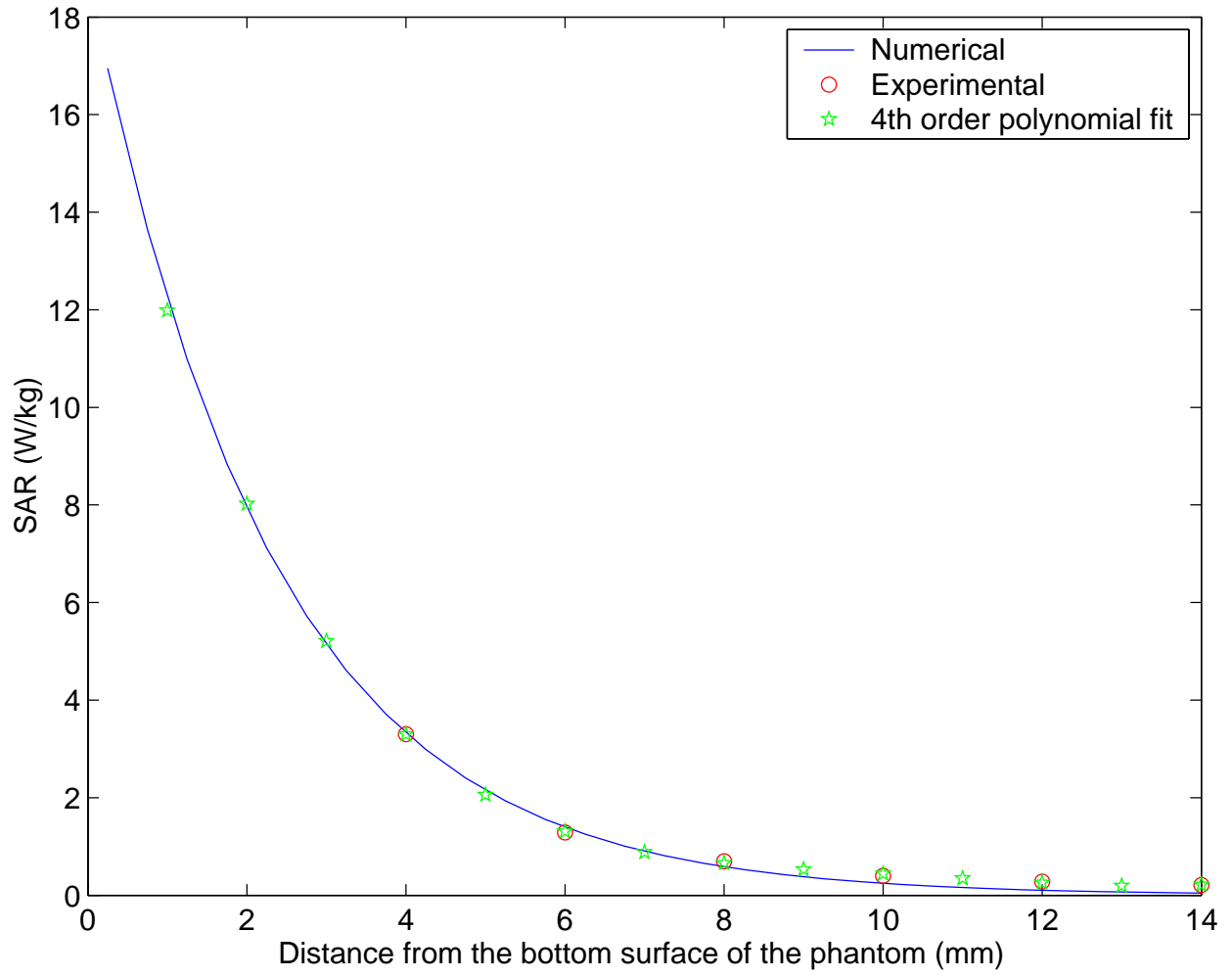
Fig. 10. The microwave circuit arrangement used for SAR system verification.



a. 5.25 GHz.

Fig. 11. Experimentally measured, extrapolated and FDTD-calculated variation of the SAR with depth in the body-simulant planar phantom. Radiated power = 100 mW.



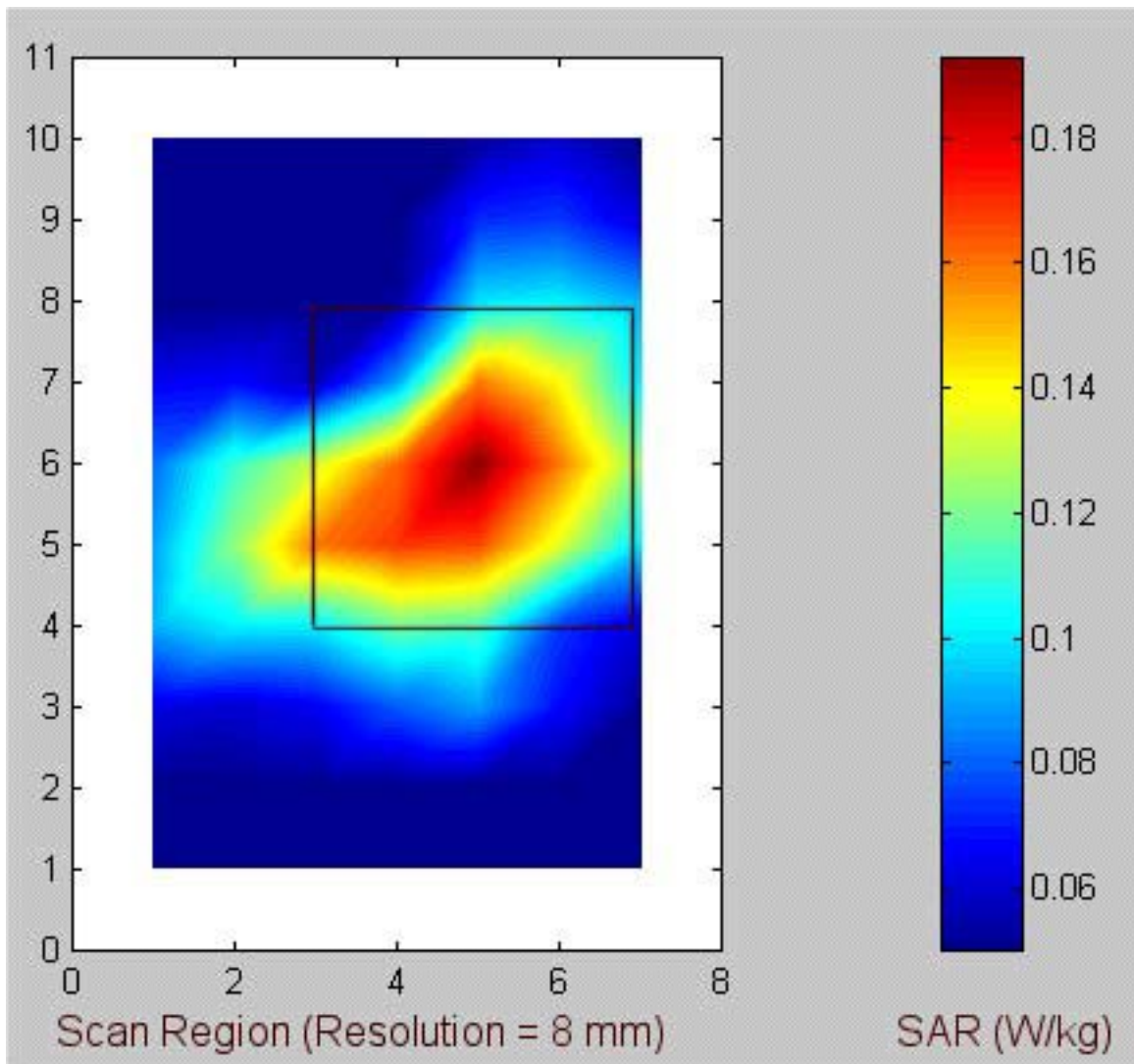


b. 5.80 GHz.

Fig. 11. Experimentally measured, extrapolated and FDTD-calculated variation of the SAR with depth in the body-simulant planar phantom. Radiated power = 100 mW.

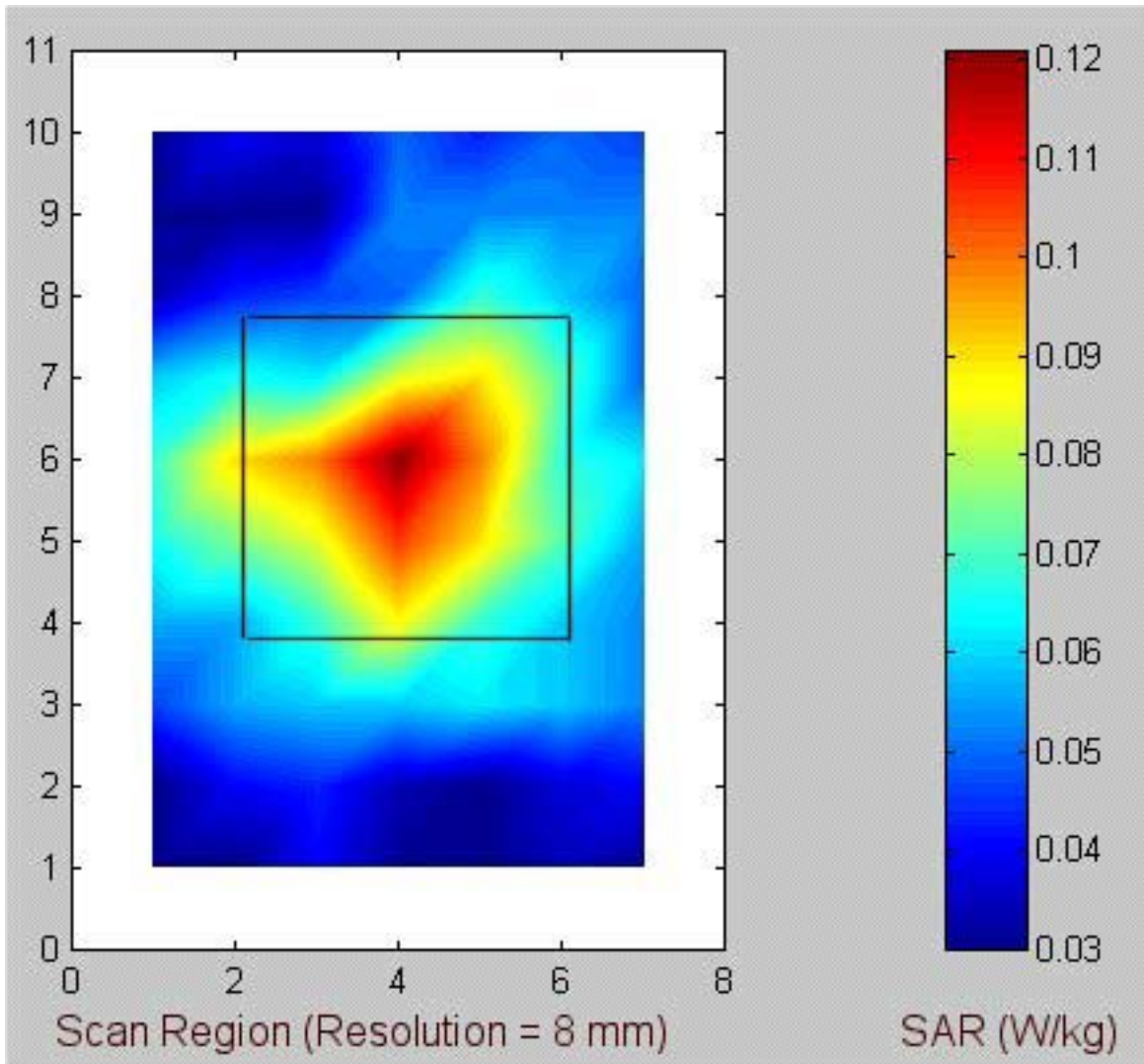


Fig. 12. Photograph of the Hewlett Packard Model 85070B Dielectric Probe. This is an open-circuited coaxial line probe.



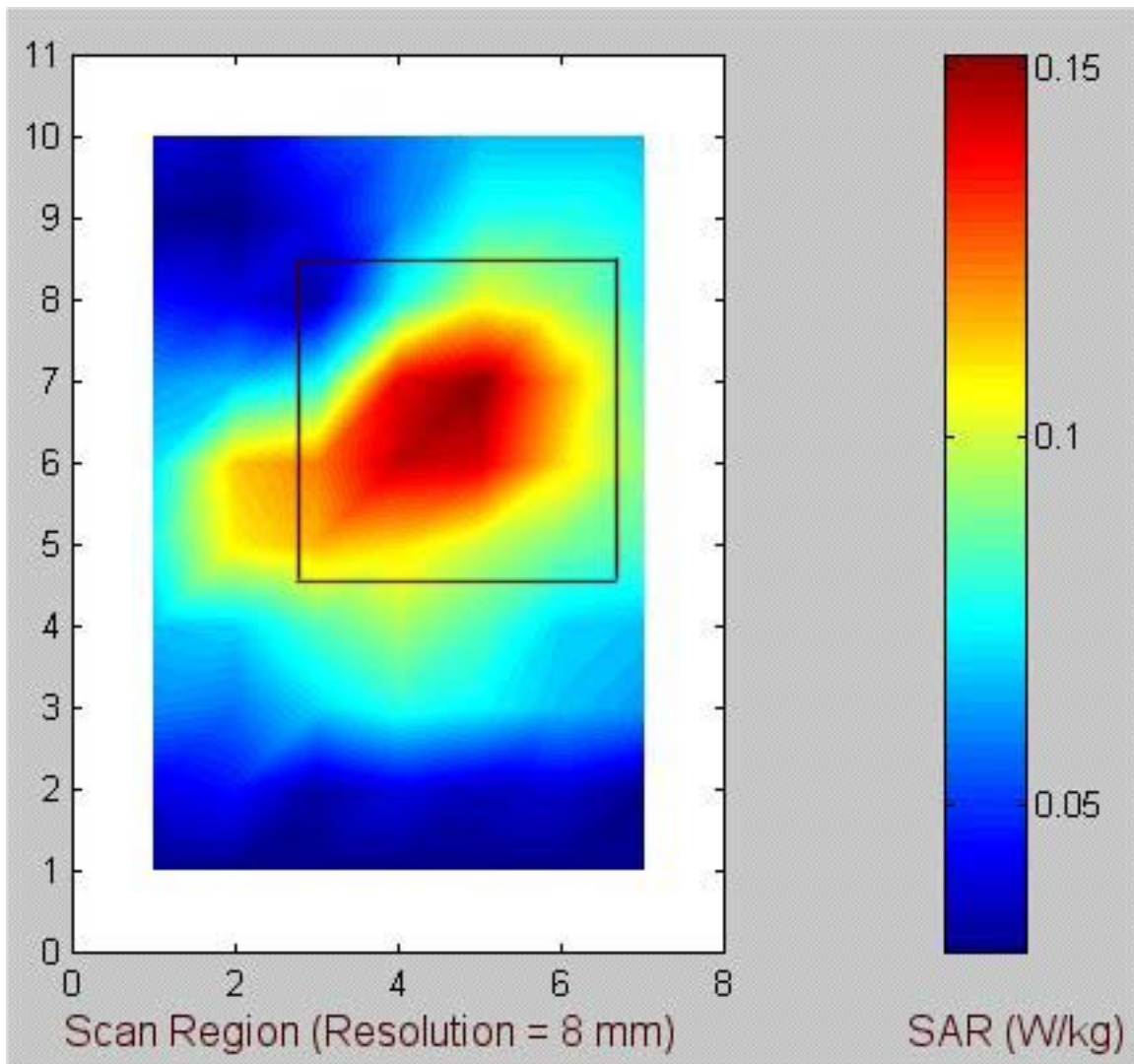
a. 5.26 GHz normal mode – antenna "A" (see Table 3 for the peak 1-g SAR).

Fig. 13. Coarse scans for the SAR measurements for antenna "A" for the **Lap-top position** of the PC relative to the flat phantom (Configuration 1, see Fig. 3a). Also shown is the antenna outline overlaid on the SAR contours. The bottom right half of the PC with antenna "A" is pressed against the base of the planar phantom.



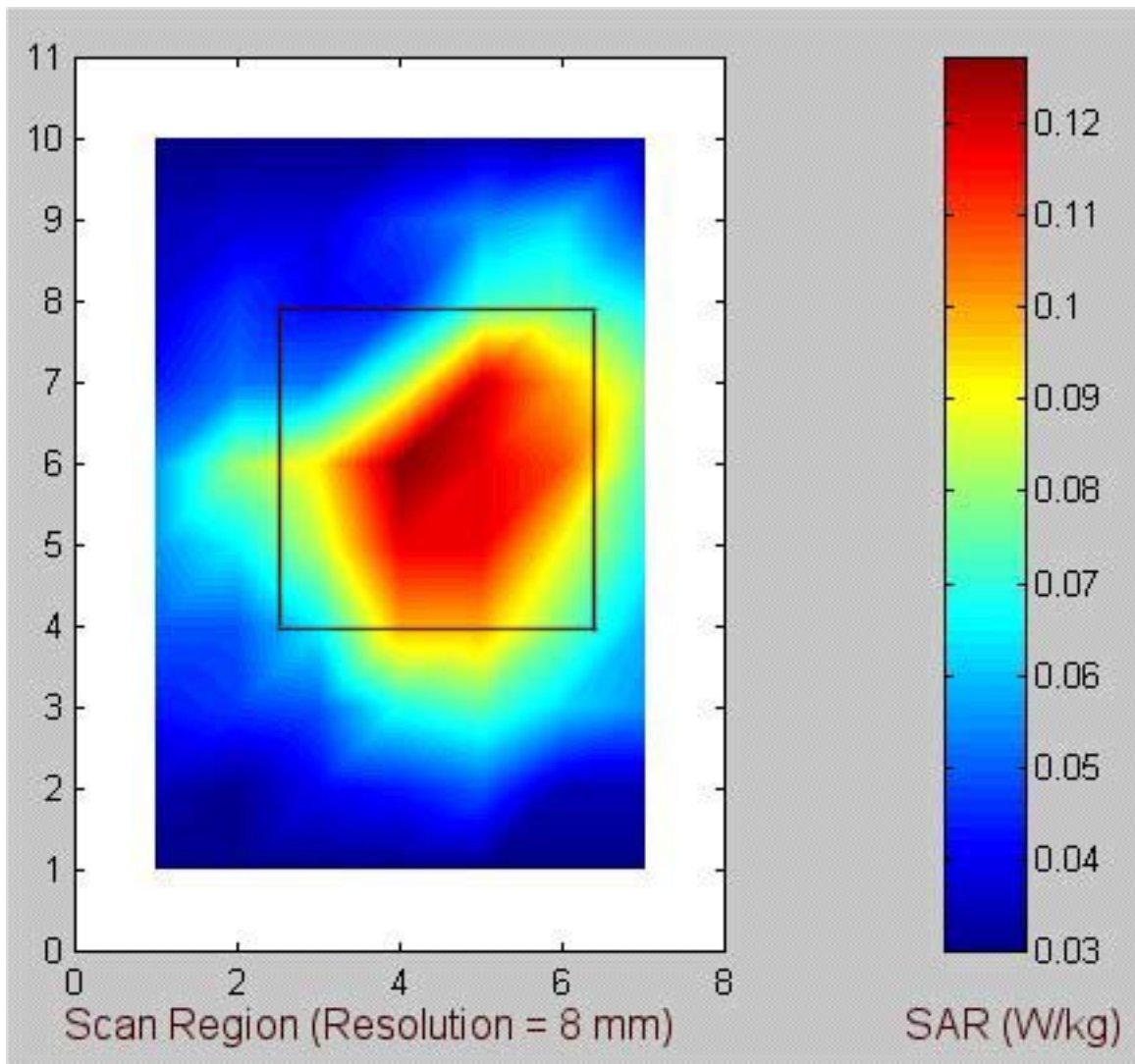
b. 5.805 GHz normal mode – antenna "A" (see Table 4 for the peak 1-g SAR).

Fig. 13. Coarse scans for the SAR measurements for antenna "A" for the **Lap-top position** of the PC relative to the flat phantom (Configuration 1, see Fig. 3a). Also shown is the antenna outline overlaid on the SAR contours. The bottom right half of the PC with antenna "A" is pressed against the base of the planar phantom.



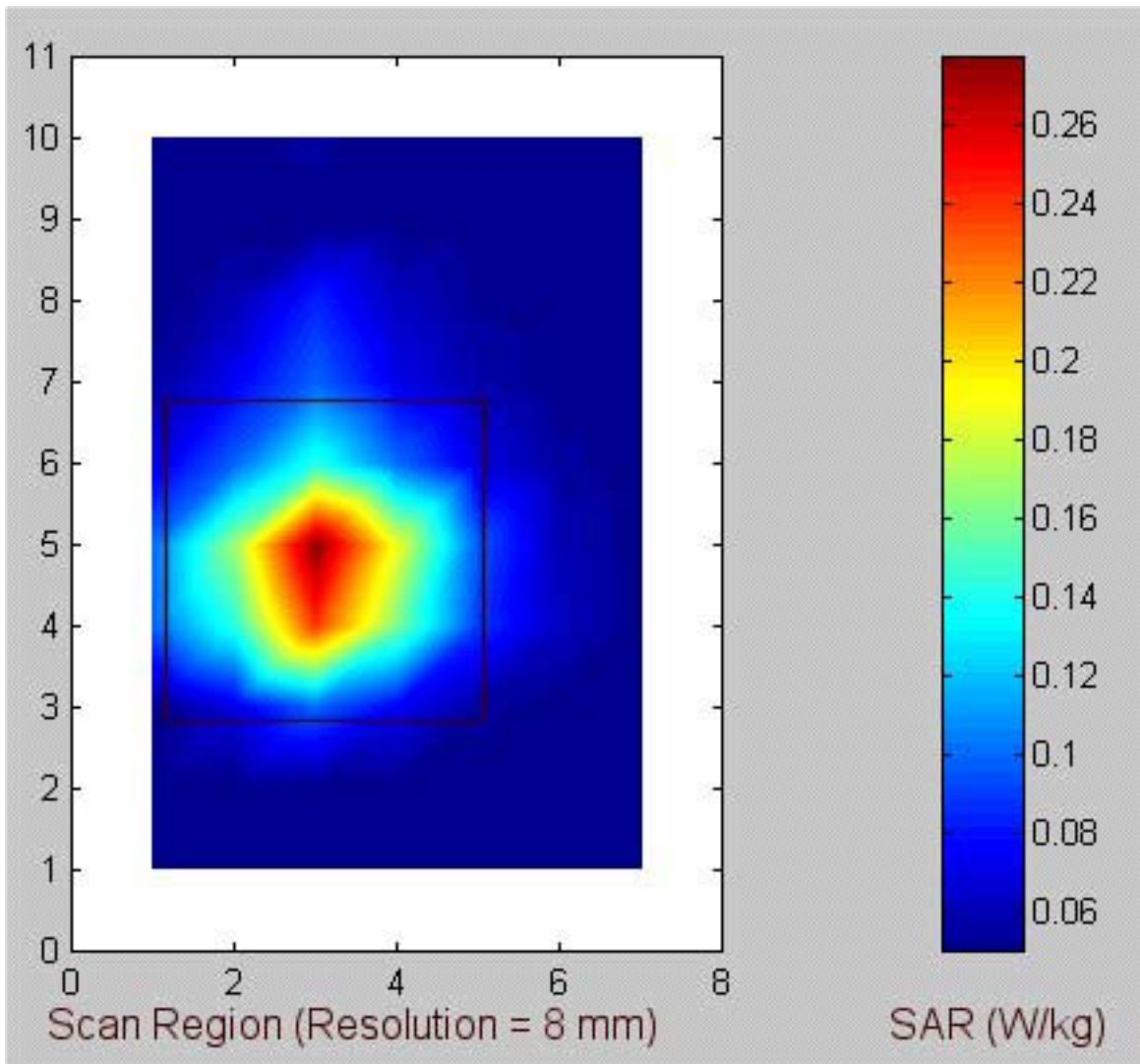
c. 5.29 GHz turbo mode – antenna "A" (see Table 5 for the peak 1-g SAR).

Fig. 13. Coarse scans for the SAR measurements for antenna "A" for the **Lap-top position** of the PC relative to the flat phantom (Configuration 1, see Fig. 3a). Also shown is the antenna outline overlaid on the SAR contours. The bottom right half of the PC with antenna "A" is pressed against the base of the planar phantom.



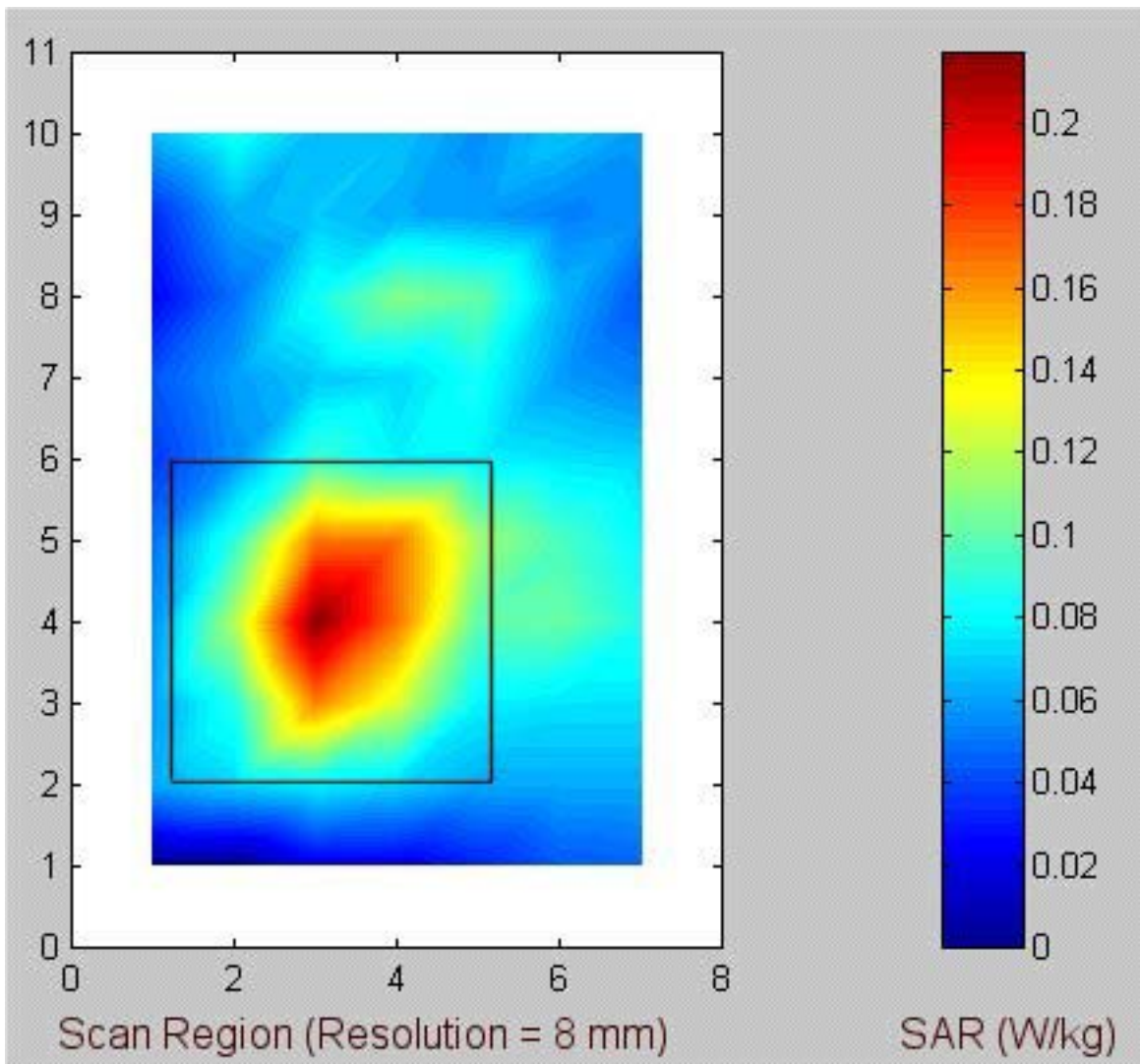
d. 5.76 GHz turbo mode – antenna "A" (see Table 6 for the peak 1-g SAR).

Fig. 13. Coarse scans for the SAR measurements for antenna "A" for the **Lap-top position** of the PC relative to the flat phantom (Configuration 1, see Fig. 3a). Also shown is the antenna outline overlaid on the SAR contours. The bottom right half of the PC with antenna "A" is pressed against the base of the planar phantom.



a. 5.26 GHz normal mode – antenna "B" (see Table 7 for the peak 1-g SAR).

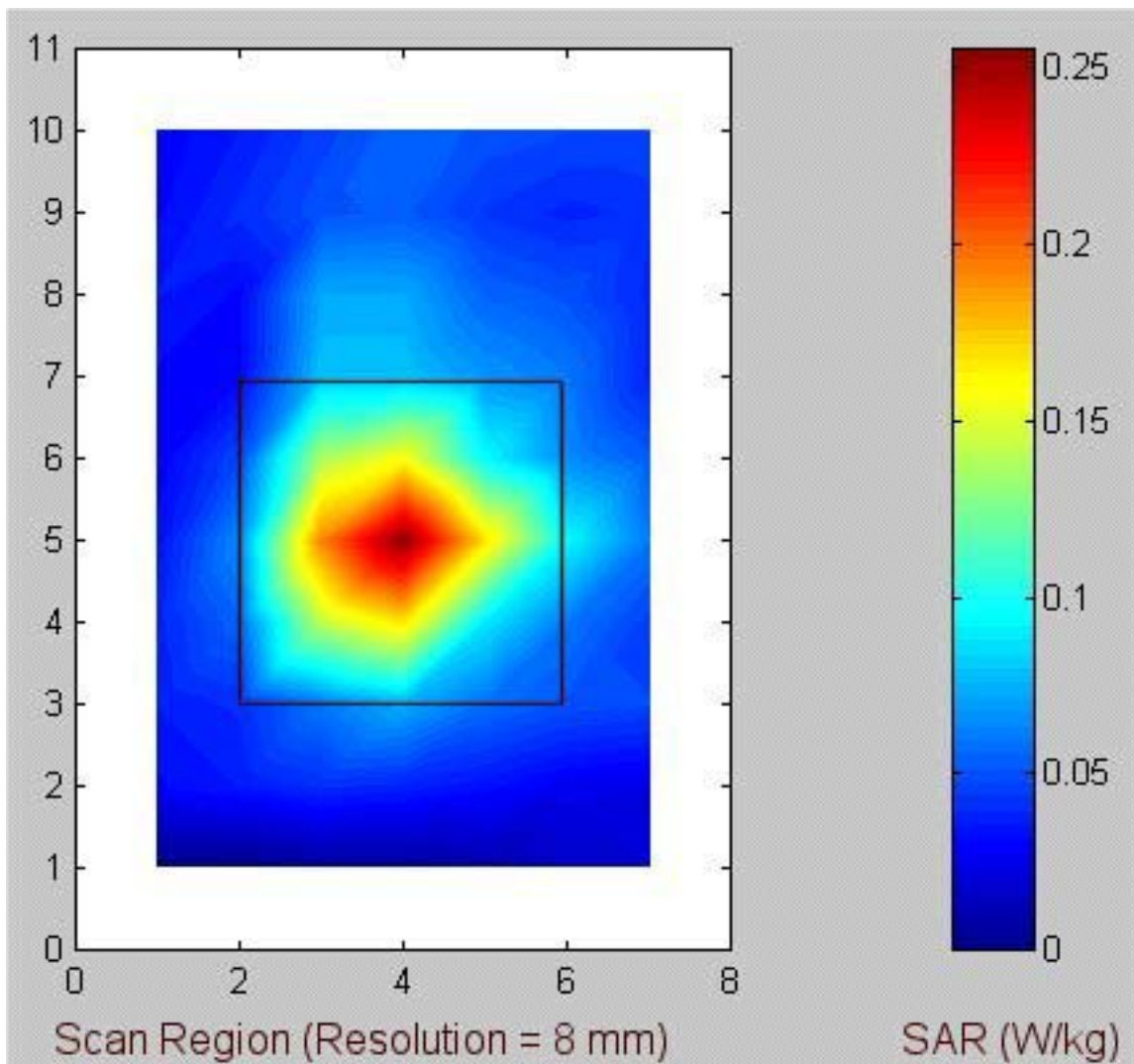
Fig. 14. Coarse scans for the SAR measurements for antenna "B" for the **Lap-top position** of the PC relative to the flat phantom (Configuration 1, see Fig. 3b). Also shown is the antenna outline overlaid on the SAR contours. The bottom right half of the PC with antenna "B" is pressed against the base of the planar phantom.



b. 5.805 GHz normal mode – antenna "B" (see Table 8 for the peak 1-g SAR).

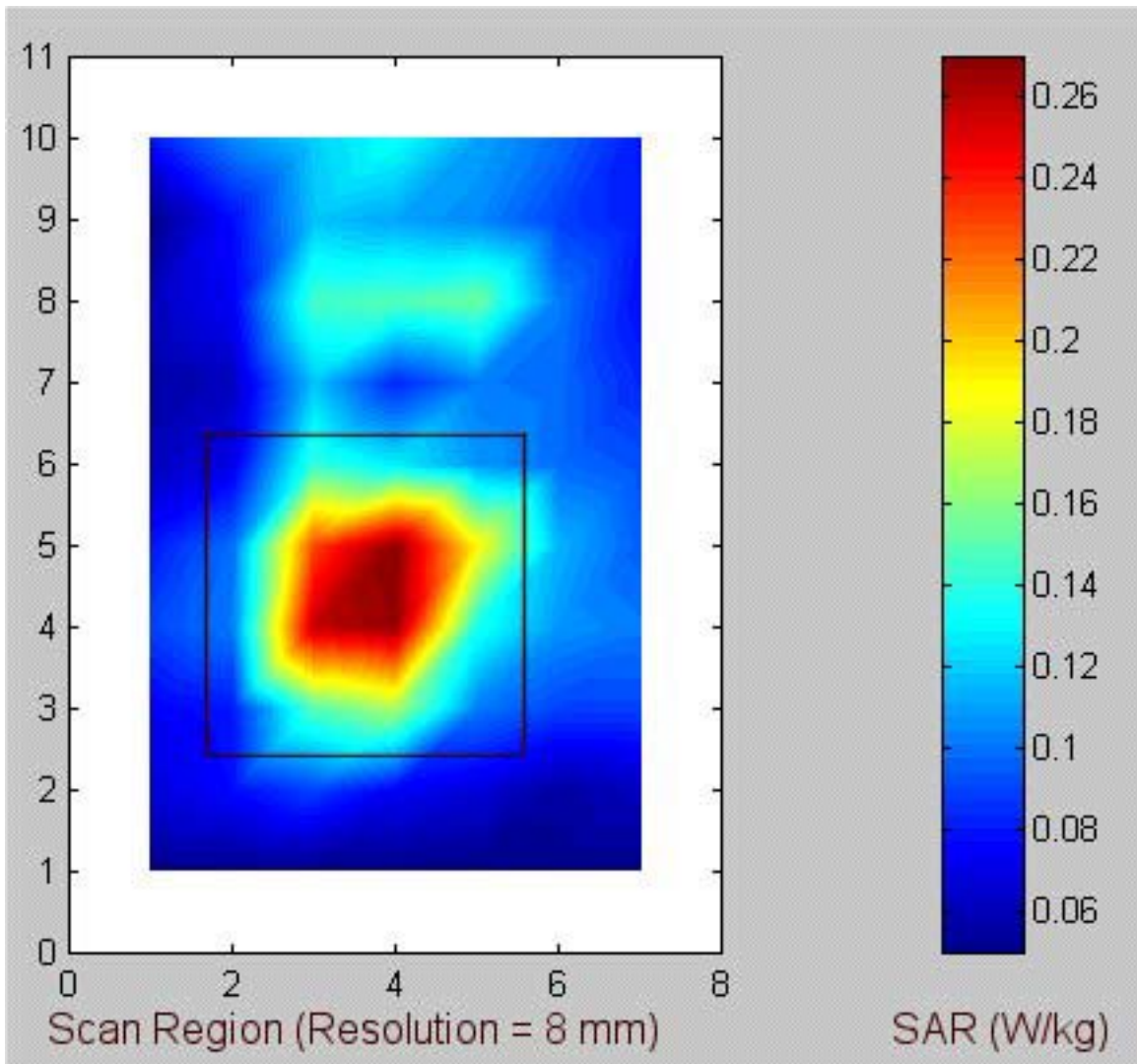
Fig. 14. Coarse scans for the SAR measurements for antenna "B" for the **Lap-top position** of the PC relative to the flat phantom (Configuration 1, see Fig. 3b). Also shown is the antenna outline overlaid on the SAR contours. The bottom right half of the PC with antenna "B" is pressed against the base of the planar phantom.





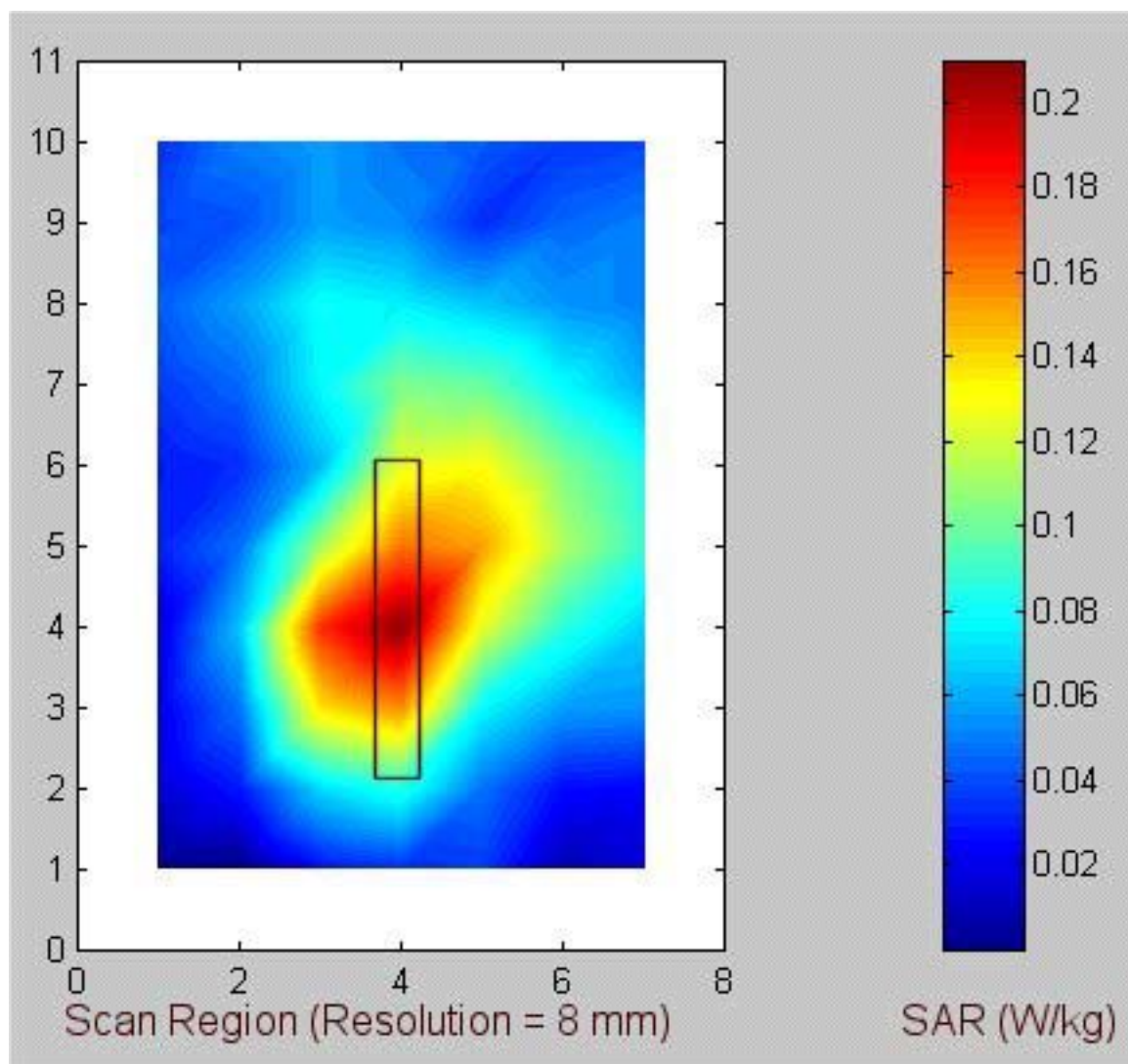
c. 5.29 GHz turbo mode – antenna "B" (see Table 9 for the peak 1-g SAR).

Fig. 14. Coarse scans for the SAR measurements for antenna "B" for the **Lap-top position** of the PC relative to the flat phantom (Configuration 1, see Fig. 3b). Also shown is the antenna outline overlaid on the SAR contours. The bottom right half of the PC with antenna "B" is pressed against the base of the planar phantom.



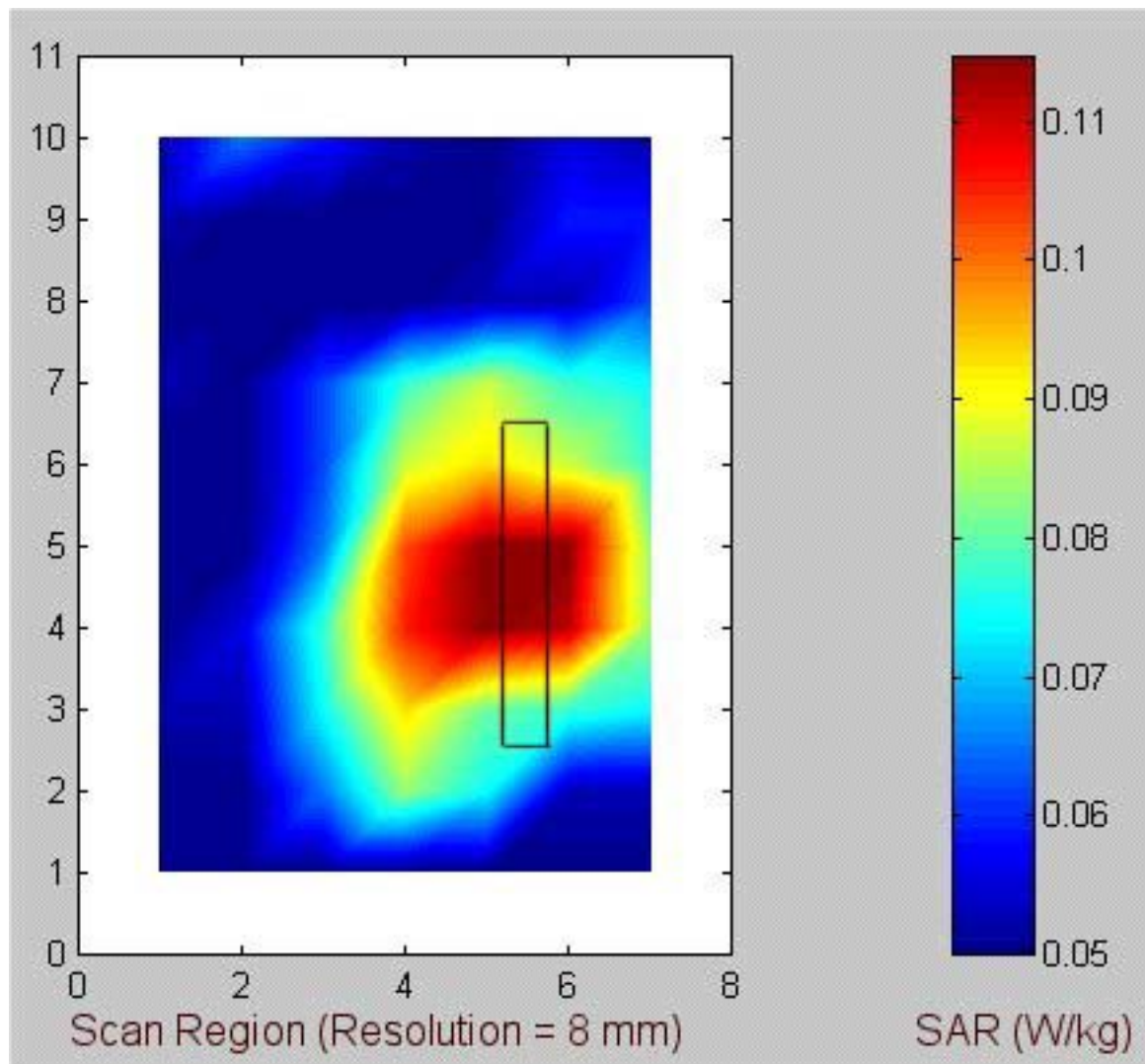
d. 5.76 GHz turbo mode – antenna "B" (see Table 10 for the peak 1-g SAR).

Fig. 14. Coarse scans for the SAR measurements for antenna "B" for the **Lap-top position** of the PC relative to the flat phantom (Configuration 1, see Fig. 3b). Also shown is the antenna outline overlaid on the SAR contours. The bottom right half of the PC with antenna "B" is pressed against the base of the planar phantom.



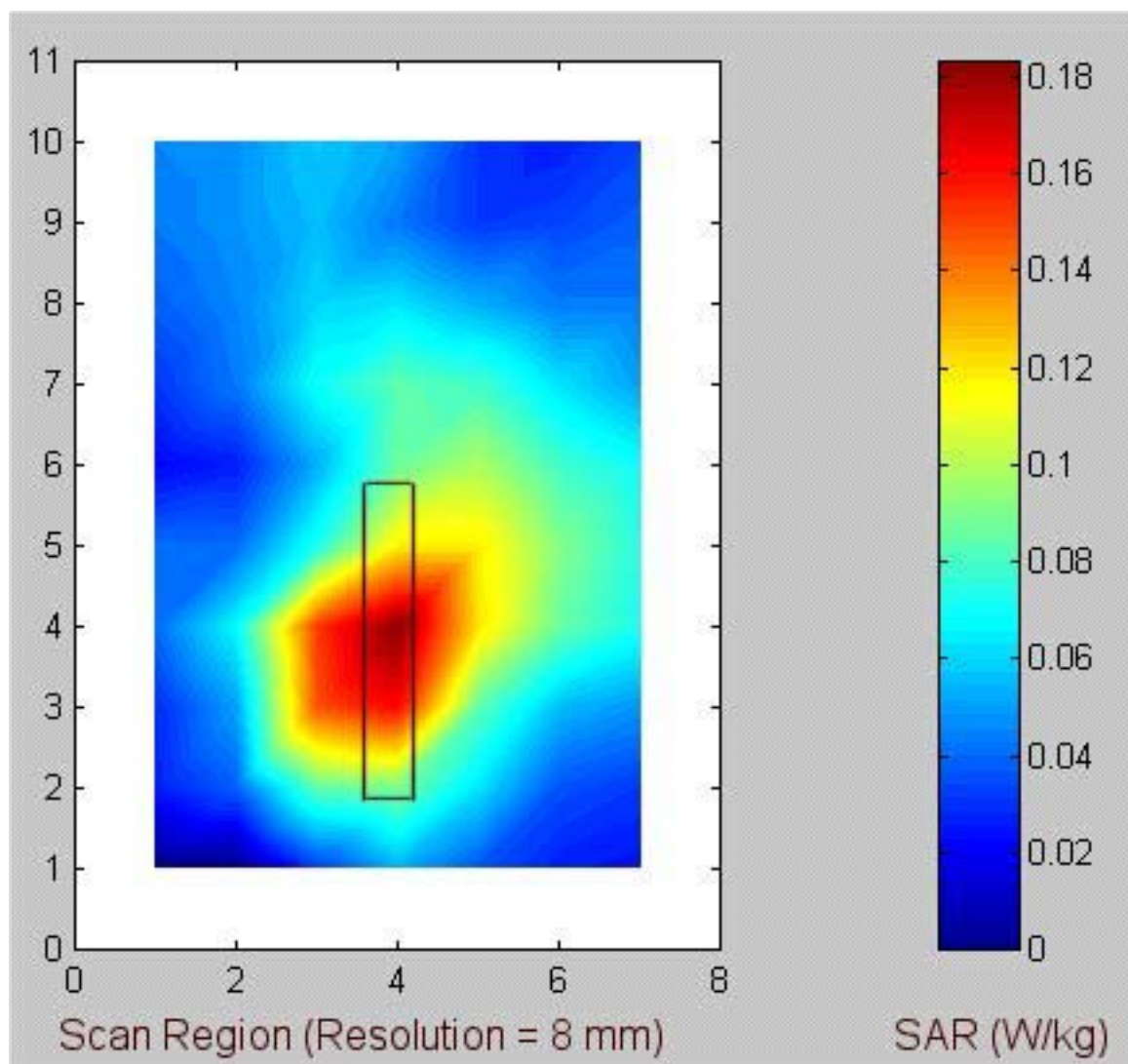
a. 5.26 GHz normal mode – antenna "A" (see Table 11 for the peak 1-g SAR).

Fig. 15. Coarse scans for the SAR measurements for the right side **Edge-on position** of the PC relative to the flat phantom (Configuration 2, see Fig. 4a). Also shown is the antenna outline overlaid on the SAR contours. The right edge of the PC with antenna "A" was placed at  $90^\circ$  at a distance of 1.5 cm from the bottom of the flat phantom.



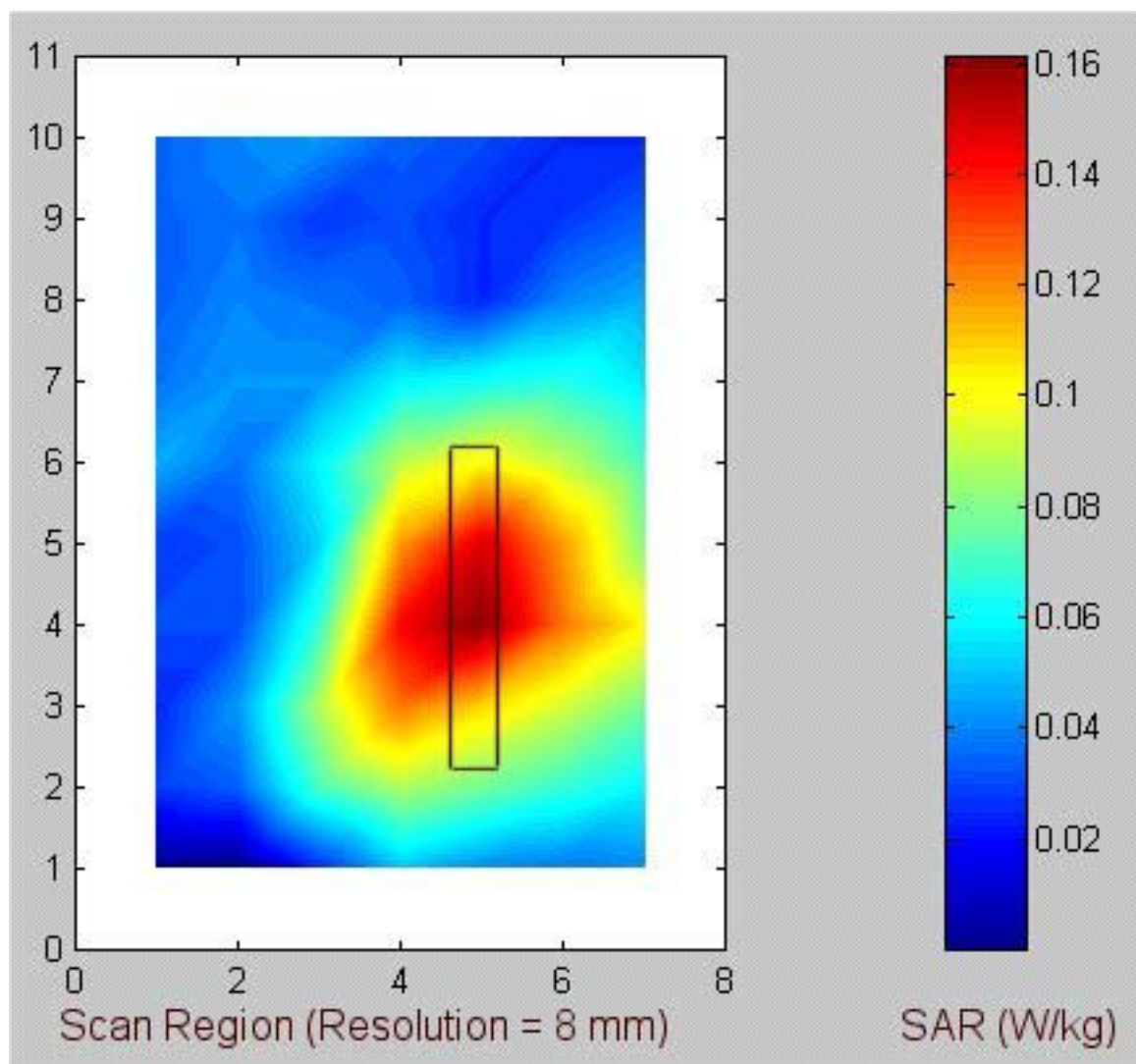
b. 5.805 GHz normal mode – antenna "A" (see Table 12 for the peak 1-g SAR).

Fig. 15. Coarse scans for the SAR measurements for the right side **Edge-on position** of the PC relative to the flat phantom (Configuration 2, see Fig. 4a). Also shown is the antenna outline overlaid on the SAR contours. The right edge of the PC with antenna "A" was placed at  $90^\circ$  at a distance of 1.5 cm from the bottom of the flat phantom.



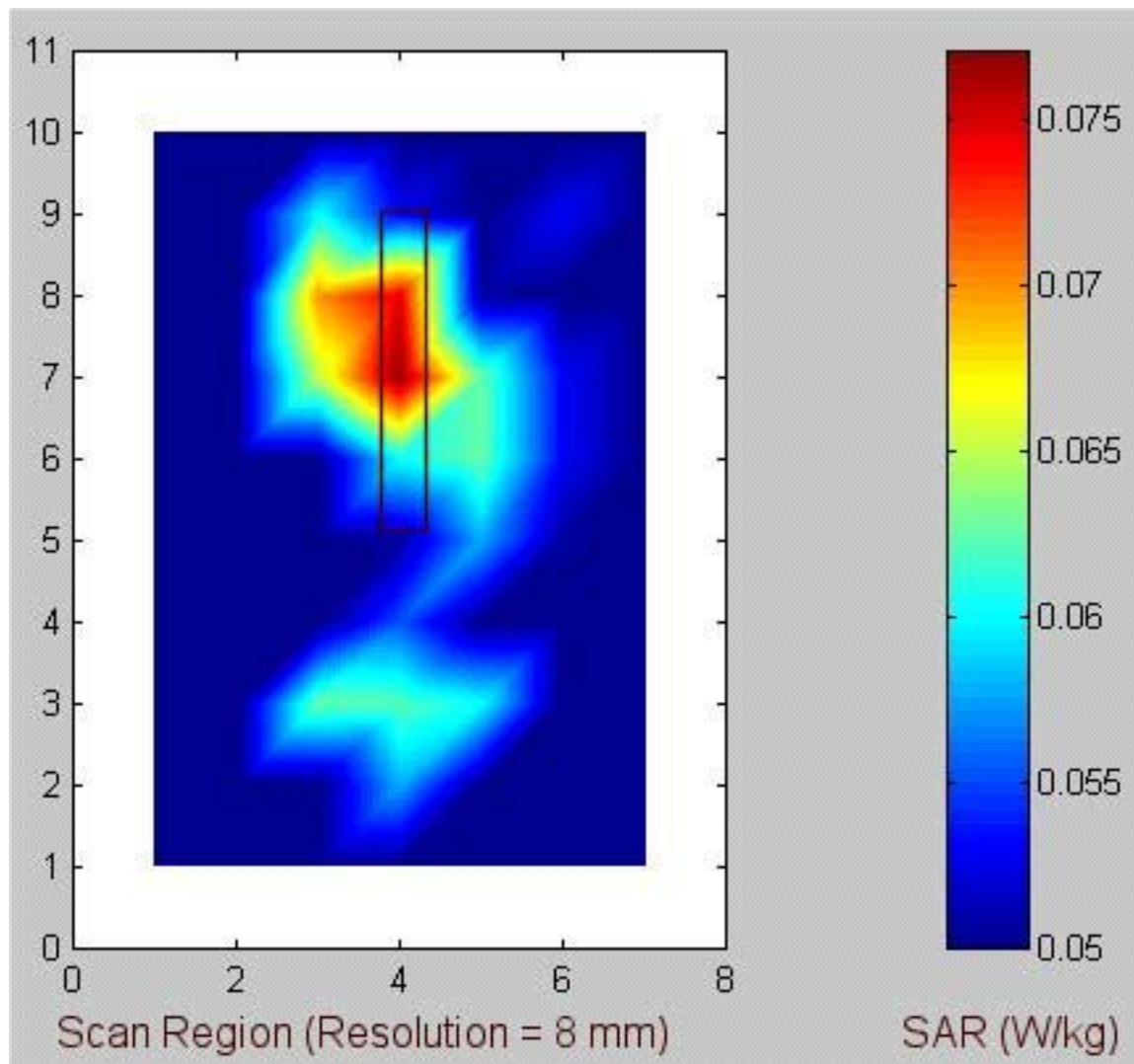
c. 5.29 GHz turbo mode – antenna "A" (see Table 13 for the peak 1-g SAR).

Fig. 15. Coarse scans for the SAR measurements for the right side **Edge-on position** of the PC relative to the flat phantom (Configuration 2, see Fig. 4a). Also shown is the antenna outline overlaid on the SAR contours. The right edge of the PC with antenna "A" was placed at  $90^\circ$  at a distance of 1.5 cm from the bottom of the flat phantom.



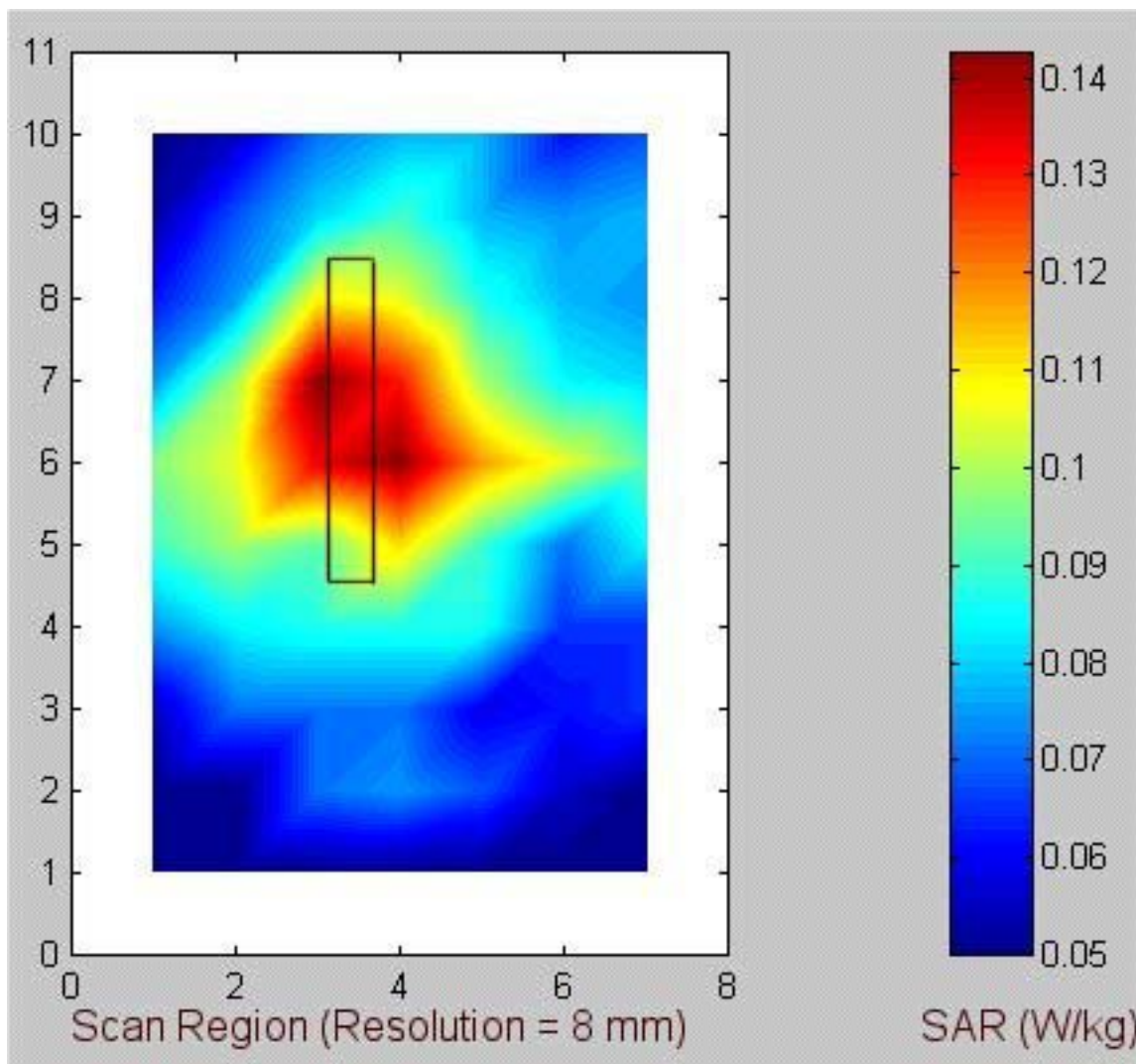
d. 5.76 GHz turbo mode – antenna "A" (see Table 14 for the peak 1-g SAR).

Fig. 15. Coarse scans for the SAR measurements for the right side **Edge-on position** of the PC relative to the flat phantom (Configuration 2, see Fig. 4a). Also shown is the antenna outline overlaid on the SAR contours. The right edge of the PC with antenna "A" was placed at  $90^\circ$  at a distance of 1.5 cm from the bottom of the flat phantom.



a. 5.26 GHz normal mode – antenna "B" (see Table 15 for the peak 1-g SAR).

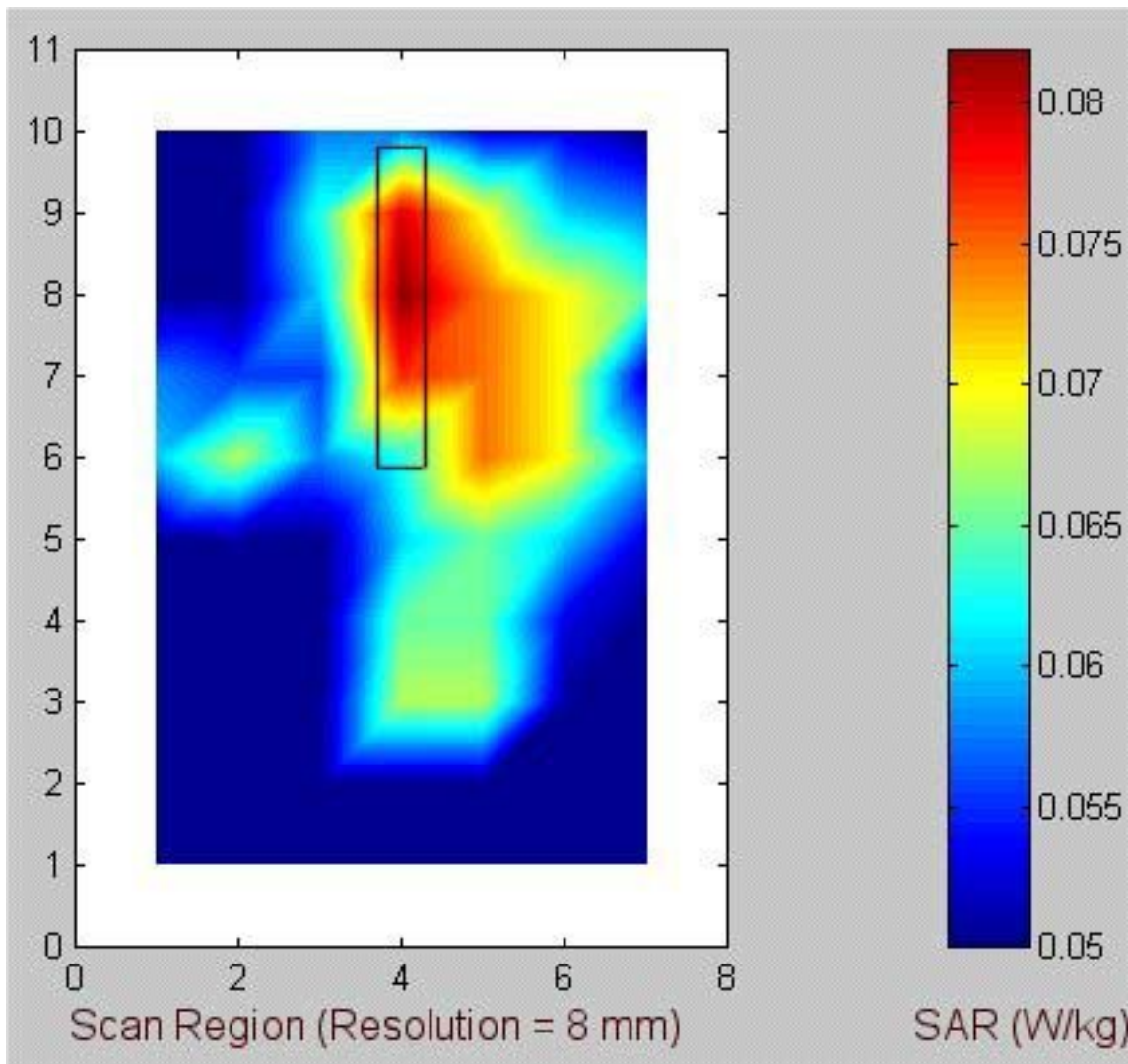
Fig. 16. Coarse scans for the SAR measurements for the left side **Edge-on position** of the PC relative to the flat phantom (Configuration 2, see Fig. 4b). Also shown is the antenna outline overlaid on the SAR contours. The left edge of the PC with antenna "B" was placed at  $90^\circ$  at a distance of 1.5 cm from the bottom of the flat phantom.



b. 5.805 GHz normal mode – antenna "B" (see Table 16 for the peak 1-g SAR).

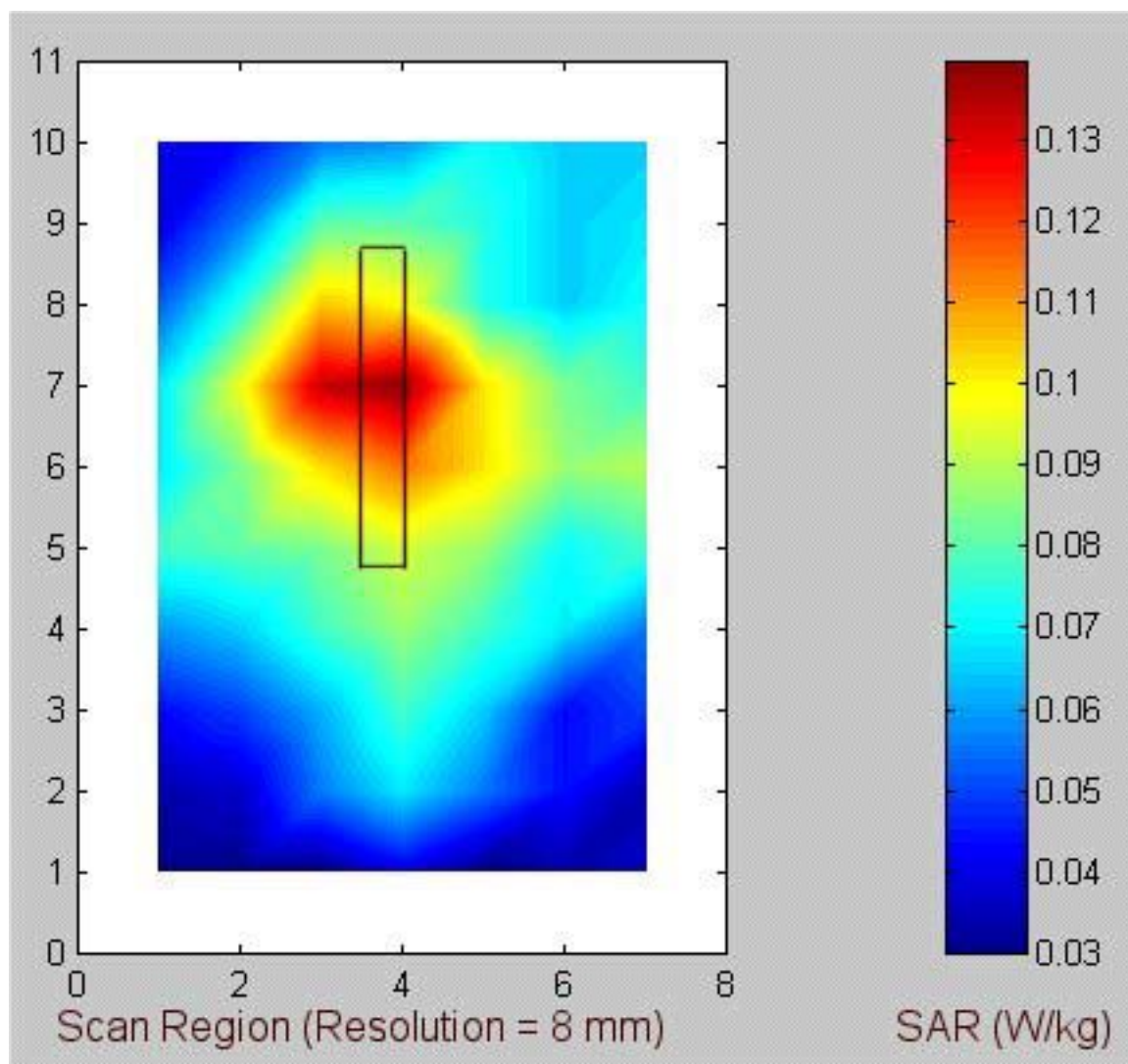
Fig. 16. Coarse scans for the SAR measurements for the left side **Edge-on position** of the PC relative to the flat phantom (Configuration 2, see Fig. 4b). Also shown is the antenna outline overlaid on the SAR contours. The left edge of the PC with antenna "B" was placed at  $90^\circ$  at a distance of 1.5 cm from the bottom of the flat phantom.





c. 5.29 GHz turbo mode – antenna "B" (see Table 17 for the peak 1-g SAR).

Fig. 16. Coarse scans for the SAR measurements for the left side **Edge-on position** of the PC relative to the flat phantom (Configuration 2, see Fig. 4b). Also shown is the antenna outline overlaid on the SAR contours. The left edge of the PC with antenna "B" was placed at  $90^\circ$  at a distance of 1.5 cm from the bottom of the flat phantom.



d. 5.76 GHz turbo mode – antenna "B" (see Table 18 for the peak 1-g SAR).

Fig. 16. Coarse scans for the SAR measurements for the left side **Edge-on position** of the PC relative to the flat phantom (Configuration 2, see Fig. 4b). Also shown is the antenna outline overlaid on the SAR contours. The left edge of the PC with antenna "B" was placed at  $90^\circ$  at a distance of 1.5 cm from the bottom of the flat phantom.

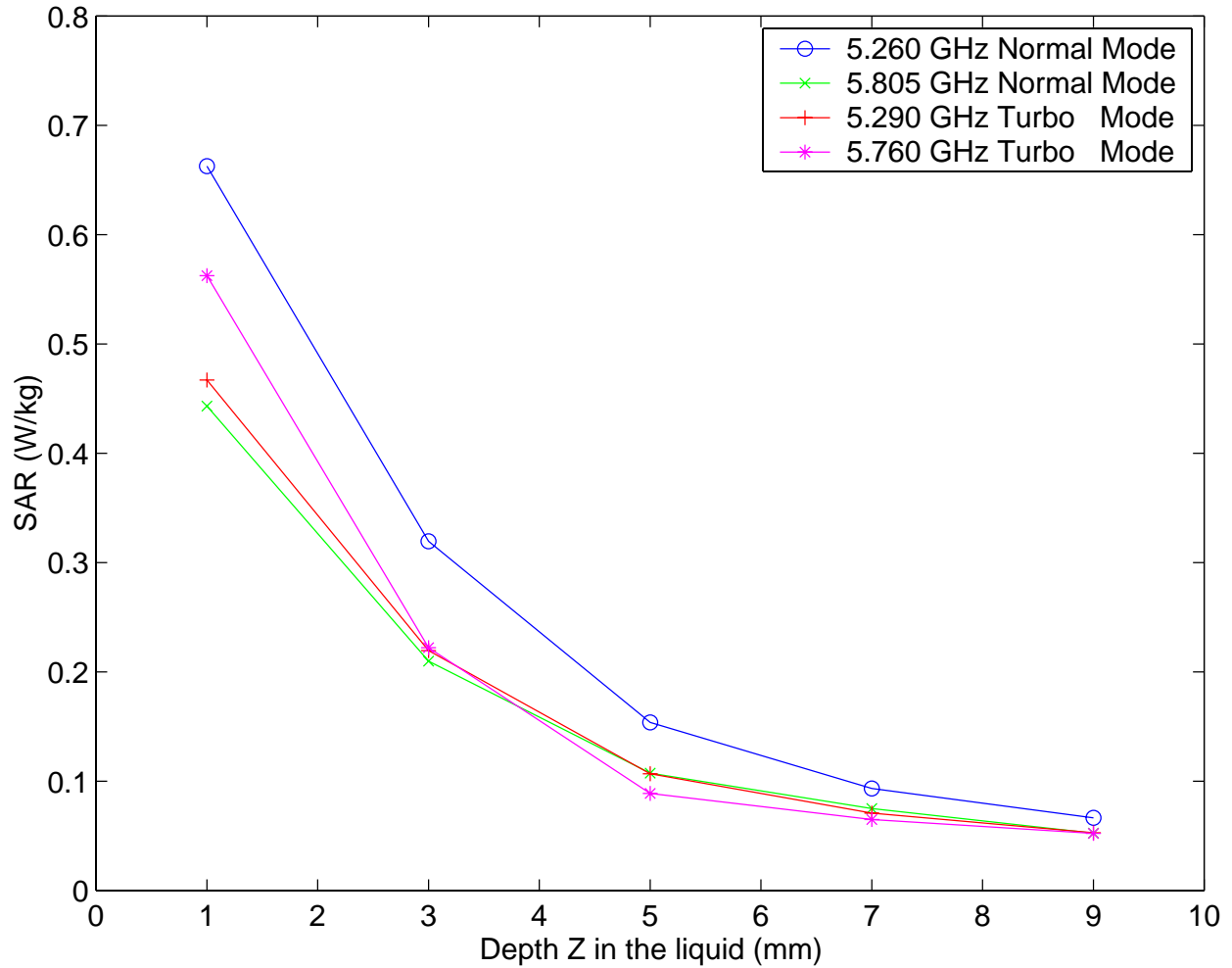


Fig. 17. Plot of the SAR variations as a function of depth Z in the liquid for locations of the highest SAR (from Tables 3-6 for **Above-lap position**) for Askey Model WLL220 Antenna "A" built into Compal Model BCL50 Notebook Computer.

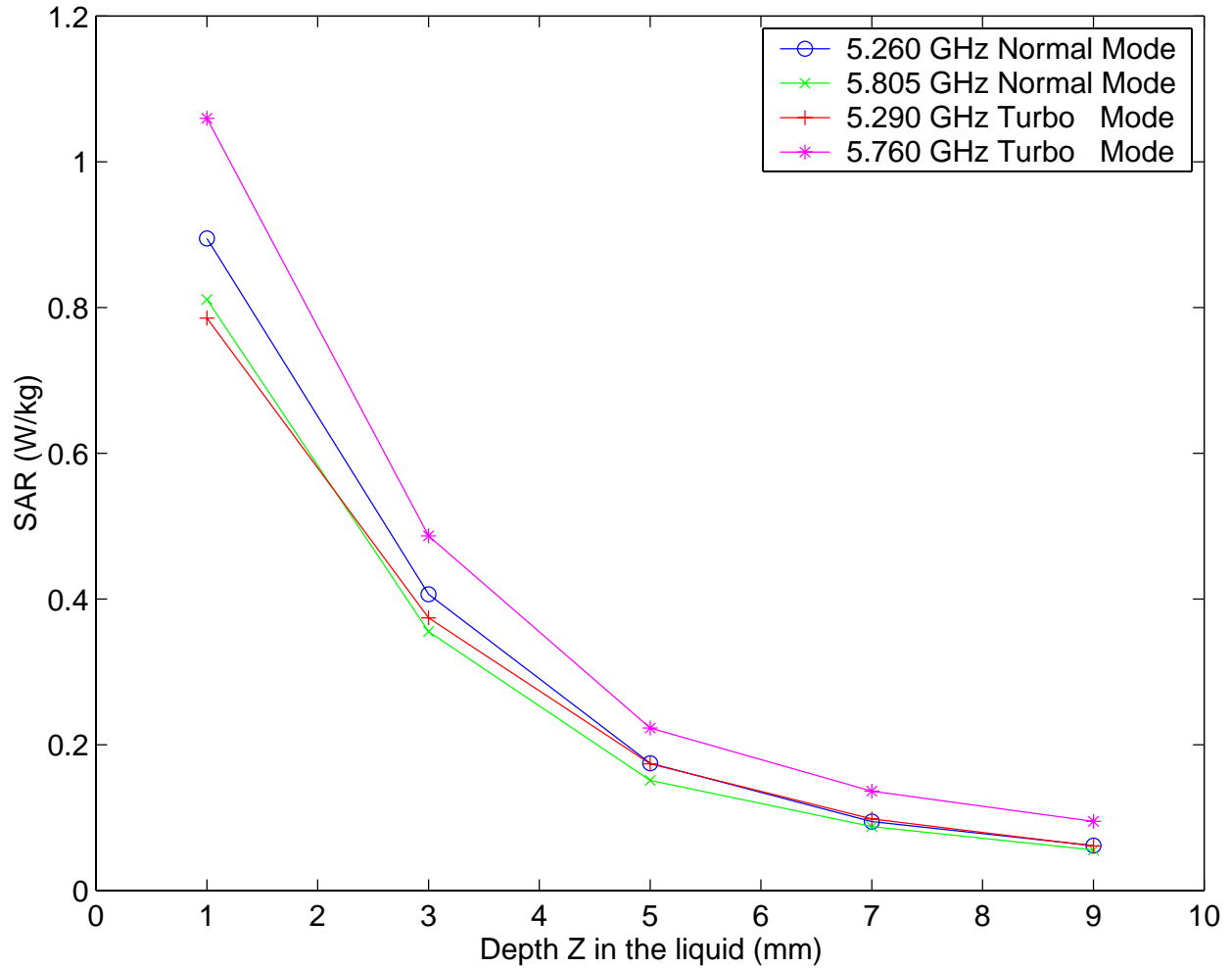


Fig. 18. Plot of the SAR variations as a function of depth Z in the liquid for locations of the highest SAR (from Tables 7-10 for **Above-lap position**) for Askey Model WLL220 Antenna "B" built into Compal Model BCL50 Notebook Computer.

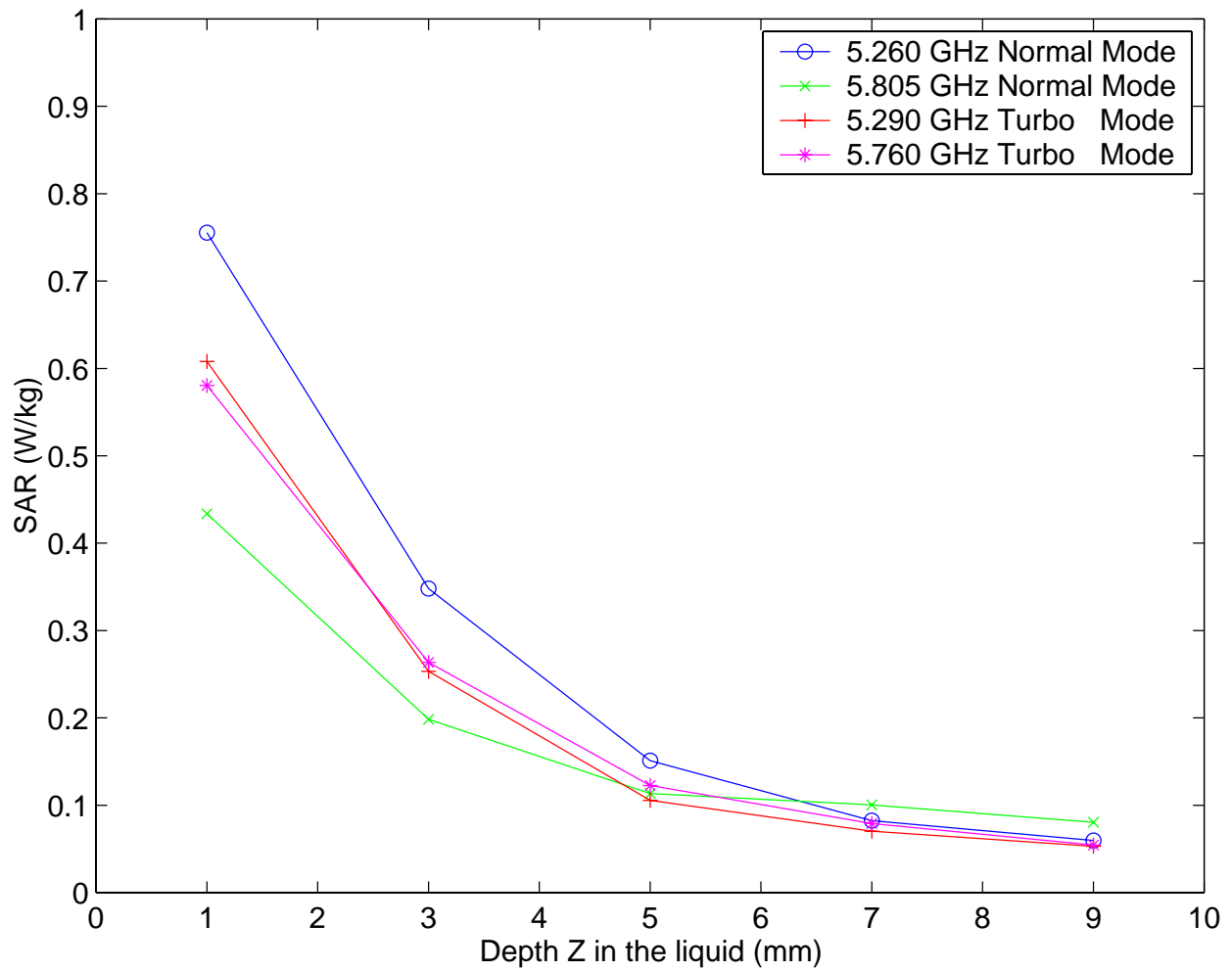


Fig. 19. Plot of the SAR variations as a function of depth Z in the liquid for locations of the highest SAR (from Tables 11-14 for **Edge-on position**) for Askey Model WLL220 Antenna "A" built into Compal Model BCL50 Notebook Computer.

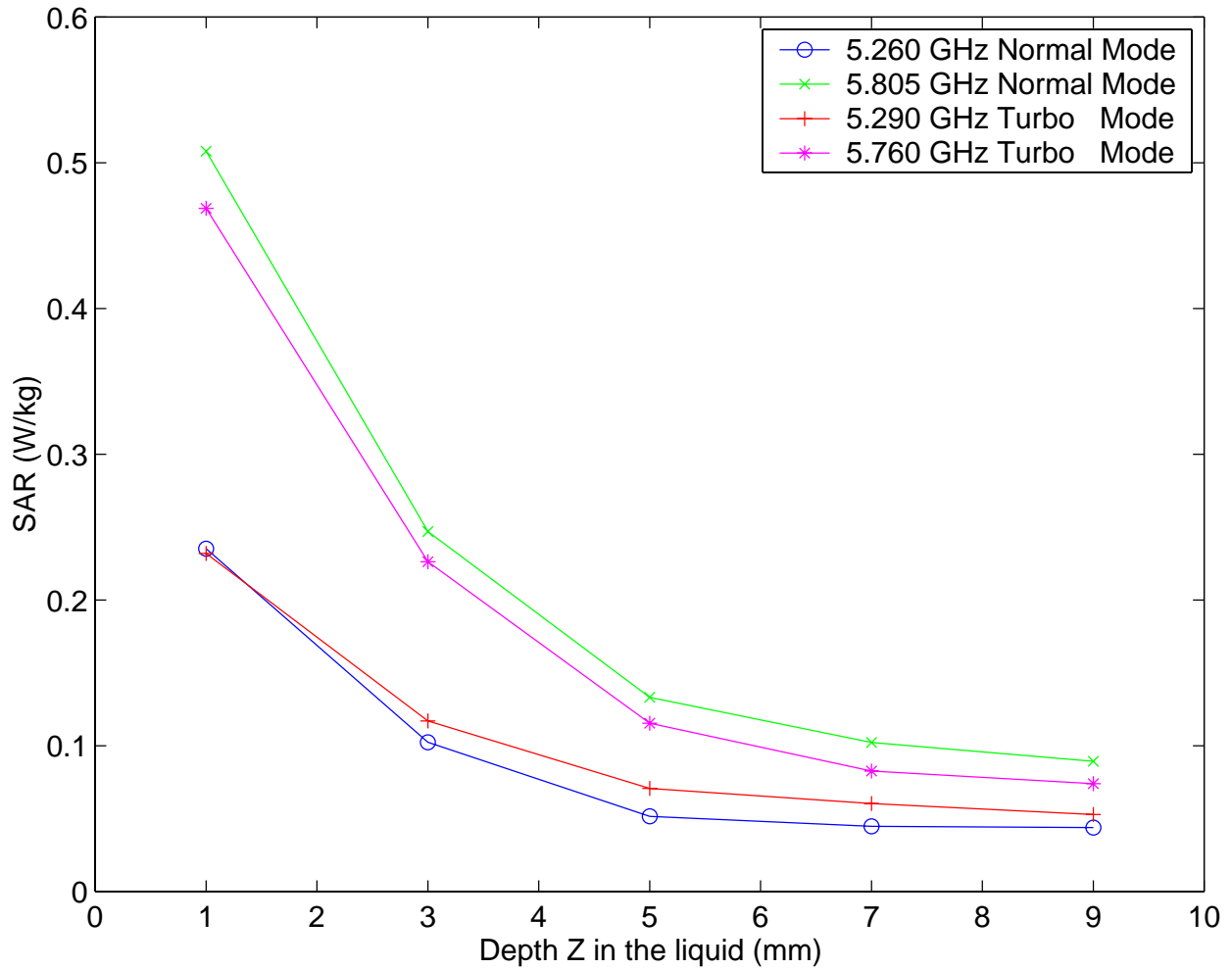


Fig. 20. Plot of the SAR variations as a function of depth Z in the liquid for locations of the highest SAR (from Tables 15-18 for **Edge-on position**) for Askey Model WLL220 Antenna "B" built into Compal Model BCL50 Notebook Computer.

APPENDIX A

SAR System Verification for April 28, 2003

The measured SAR distribution for the peak 1-g SAR region using WR187 rectangular waveguide irradiation system

For April 28, 2003 – The SAR plot at 5.25 GHz

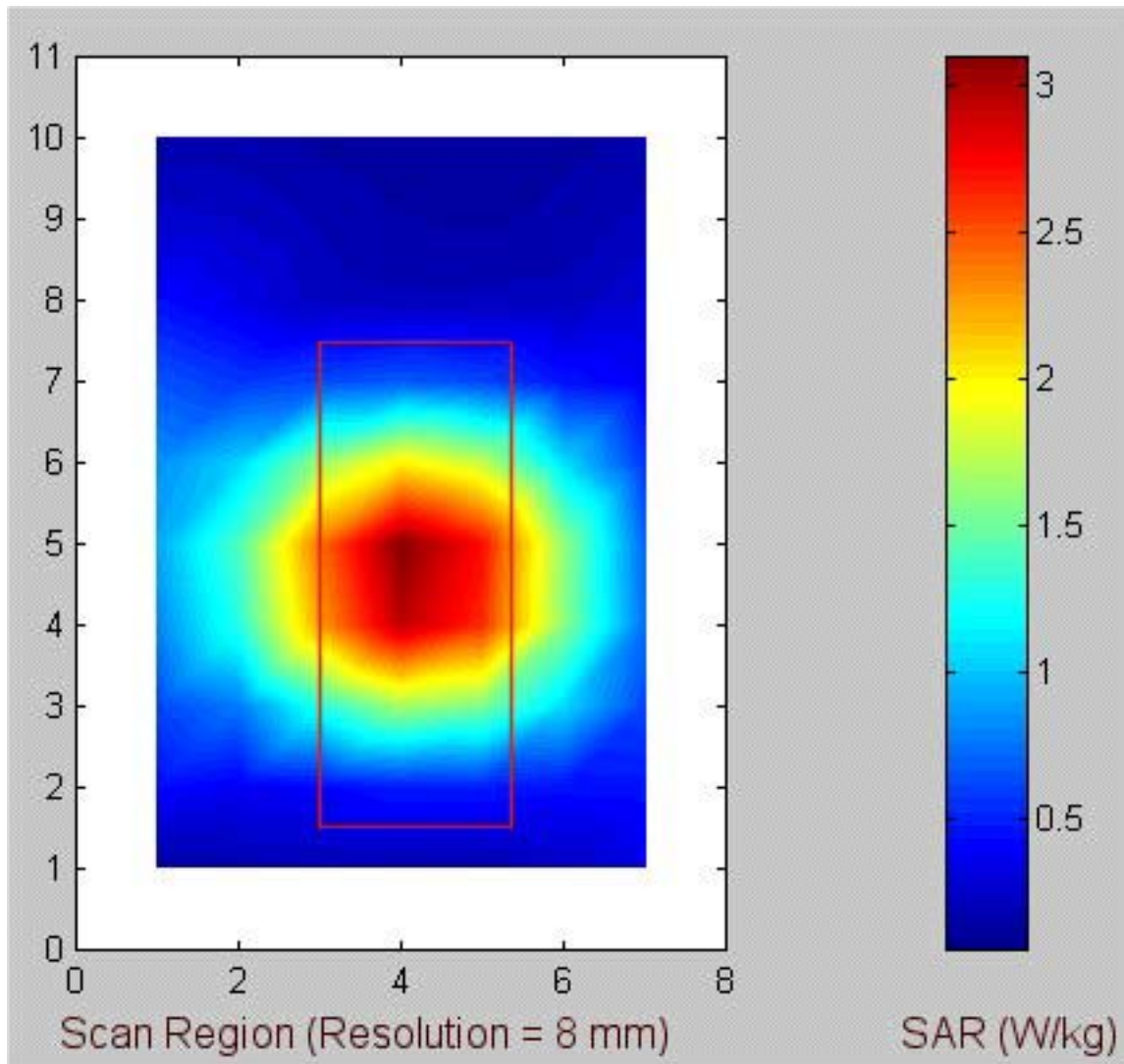


Fig. A.1. Coarse scans of the measured SAR distribution for the WR187 rectangular waveguide irradiation system used for system verification at 5.25 GHz. Also shown is the outline of the rectangular waveguide overlaid on the SAR contours. Radiated power = 100 mW.

**1-g SAR = 3.678 W/kg**

**a. At depth of 1 mm**

9.201	9.627	9.989	9.919	9.628
9.790	10.137	10.522	10.397	10.063
10.067	10.674	10.708	10.714	10.371
9.933	10.428	10.709	10.715	10.317
9.762	10.192	10.328	10.284	9.917

**b. At depth of 3 mm**

4.199	4.390	4.528	4.528	4.421
4.457	4.643	4.786	4.760	4.636
4.595	4.846	4.884	4.899	4.769
4.561	4.758	4.890	4.893	4.735
4.457	4.645	4.731	4.719	4.575

**c. At depth of 5 mm**

1.822	1.903	1.943	1.969	1.925
1.923	2.013	2.068	2.066	2.029
1.983	2.086	2.113	2.123	2.076
1.978	2.052	2.116	2.113	2.058
1.931	2.002	2.061	2.063	2.006

**d. At depth of 7 mm**

0.878	0.916	0.923	0.950	0.920
0.916	0.960	0.988	0.986	0.972
0.939	0.998	1.009	1.010	0.987
0.936	0.973	1.007	1.000	0.979
0.926	0.953	0.993	0.997	0.968

**e. At depth of 9 mm**

0.539	0.560	0.558	0.581	0.554
0.555	0.583	0.594	0.595	0.583
0.565	0.610	0.612	0.604	0.590
0.559	0.590	0.604	0.595	0.586
0.568	0.586	0.604	0.604	0.593



For April 28, 2003 – The SAR plot at 5.8 GHz

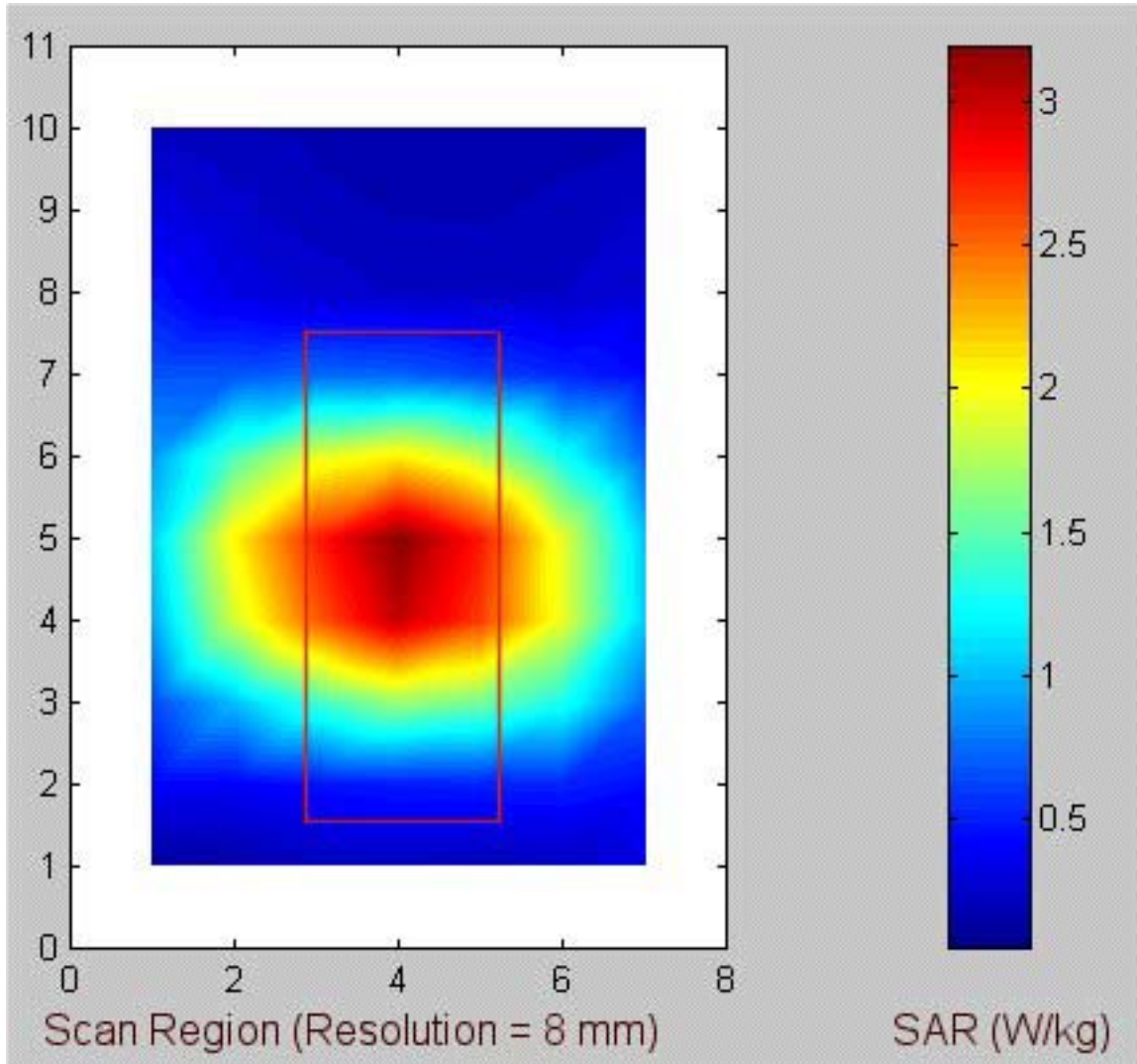


Fig. A.2. Coarse scans of the measured SAR distribution for the WR187 rectangular waveguide irradiation system used for system verification at 5.8 GHz. Also shown is the outline of the rectangular waveguide overlaid on the SAR contours. Radiated power = 100 mW.

1-g SAR = 3.947 W/kg

**a. At depth of 1 mm**

10.705	11.116	11.054	11.024	10.620
11.337	11.704	11.800	11.627	10.982
11.543	11.928	11.988	11.877	11.132
11.653	12.027	11.862	11.680	11.311
11.212	11.550	11.669	11.304	10.889

**b. At depth of 3 mm**

4.677	4.814	4.821	4.794	4.649
4.908	5.072	5.128	5.020	4.795
5.001	5.173	5.211	5.129	4.899
5.032	5.180	5.182	5.072	4.905
4.848	4.983	5.030	4.906	4.729

**c. At depth of 5 mm**

1.885	1.910	1.931	1.911	1.870
1.945	2.006	2.041	1.980	1.928
1.979	2.044	2.061	2.022	1.971
1.985	2.035	2.064	2.007	1.945
1.916	1.969	1.983	1.951	1.886

**d. At depth of 7 mm**

0.845	0.840	0.855	0.841	0.826
0.851	0.873	0.890	0.859	0.856
0.862	0.882	0.884	0.874	0.857
0.867	0.879	0.889	0.864	0.849
0.835	0.864	0.864	0.857	0.834

**e. At depth of 9 mm**

0.528	0.521	0.531	0.518	0.504
0.520	0.538	0.535	0.520	0.524
0.525	0.534	0.530	0.523	0.514
0.538	0.527	0.529	0.517	0.519
0.511	0.532	0.526	0.528	0.516

## APPENDIX B

### **Uncertainty Analysis**

The uncertainty analysis of the University of Utah SAR Measurement System is given in Table B.1. Several of the numbers on tolerances are obtained by following procedures similar to those detailed in [8], while others have been obtained using methods suggested in [4].

Table B.1. Uncertainty analysis of the University of Utah SAR Measurement System.

Uncertainty Component	Tolerance ± %	Prob. Dist.	Div.	C <sub>i</sub> 1-g	1-g u <sub>i</sub> ± %
<b>Measurement System</b>					
Probe calibration	2.0	N	1	1	2.0
Axial isotropy	4.0	R	$\sqrt{3}$	$(1-c_p)^{1/2}$	1.6
Hemispherical isotropy	5.5	R	$\sqrt{3}$	$\sqrt{c_p}$	0.0
Boundary effect	0.8	R	$\sqrt{3}$	1	0.5
Linearity	3.0	R	$\sqrt{3}$	1	1.7
System detection limits	1.0	R	$\sqrt{3}$	1	0.6
Readout electronics	1.0	N	1	1	1.0
Response time	0.0	R	$\sqrt{3}$	1	0.0
Integration time	0.5	R	$\sqrt{3}$	1	0.3
RF ambient conditions	0	R	$\sqrt{3}$	1	0
Probe positioner mechanical tolerance	0.5	R	$\sqrt{3}$	1	0.3
Probe positioning with respect to phantom shell	2.0	R	$\sqrt{3}$	1	1.2
Extrapolation, interpolation, and integration algorithms for max. SAR evaluation	5.0	R	$\sqrt{3}$	1	2.9
<b>Test Sample Related</b>					
Test sample positioning	3	R	$\sqrt{3}$	1	1.7
Device holder uncertainty	3	R	$\sqrt{3}$	1	1.7
Output power variation - SAR drift measurement	5	R	$\sqrt{3}$	1	2.9
<b>Phantom and Tissue Parameters</b>					
Phantom uncertainty - shell thickness tolerance	10.0	R	$\sqrt{3}$	1	5.8
Liquid conductivity - deviation from target values	0.4	R	$\sqrt{3}$	0.7	0.2
Liquid conductivity - measurement uncertainty	1.5	R	$\sqrt{3}$	0.7	0.6
Liquid permittivity - deviation from target values	0.8	R	$\sqrt{3}$	0.6	0.3
Liquid permittivity - measurement uncertainty	3.5	R	$\sqrt{3}$	0.6	1.2
<b>Combined Standard Uncertainty</b>		RSS			8.3
<b>Expanded Uncertainty (95% Confidence Level)</b>					16.6